Stability and vortex structures of quasi-two-dimensional shear flows

F. V. Dolzhanskiĭ, V. A. Krymov, and D. Yu. Manin

Institute of the Physics of the Atmosphere of the Academy of Sciences of the USSR
Usp. Fiz. Nauk **160**, 1–47 (July 1990)

This review is devoted to the theoretical description and laboratory modeling of quasi-two-dimensional shear flows (including flows in thin layers of liquid and in rotating systems). Such flows are of interest in connection with the possibility of the appearance of ordered vortex structures in them as a result of the shear instability. The main attention is devoted to theoretical models in which the friction of the liquid against the underlying surface is taken into account. Comparing the theoretical results with laboratory data shows that friction plays the decisive role in the appearance and evolution of vortex structures. As an application, the large-scale dynamics of the earth's atmosphere is studied.

INTRODUCTION

Flows of liquid or gas in which for some physical reason the horizontal component of the velocity field is much stronger than the vertical component play an important role in hydrodynamic systems in nature and in technology. Such flows include, in particular, the large-scale motions of the ocean and atmospheres of the rotating planets (including the earth), the circulation on the sun and other stars, the evolution of galaxies, and flow in a magnetized plasma. Laboratory hydrodynamic experiments, in which the indicated phenomena are modeled under controlled conditions, are substantially enlarging the class of such flows.

It should be noted that in the second half of the twentieth century laboratory hydrodynamic experiments acquired a second wind starting with the experiments of Fultz and Hide,[1,2] in which a serious attempt was made to reproduce the properties of the general circulation of the atmosphere and the convection of the liquid inner core of the earth. The laboratory experimental results obtained in geophysical hydrodynamics by the end of the 1970's are reviewed in Refs. 3 and 4. The number of publications on this subject is still increasing; this can be easily verified by looking through current physical and hydrodynamical journals and proceedings of conferences on nonlinear processes in physics and turbulence. Nezlin's review[5] recently published in Soviet Physics Uspekhi deserves special attention; it is devoted to the laboratory modeling of the so-called Rossby solitons and other phenomena observed in Jupiter's atmosphere and in galaxies (see also Ref. 6).

A component of the velocity field of a flow can be suppressed for different reasons, such as, rotation of the system as a whole, the presence of a constant magnetic field threading through an electrically conducting liquid, strong density stratification (as, for example, in the ocean), thinness of the layer of liquid in which motion develops, or a combination of these factors. We shall call motions of this type **quasi-two-dimensional**. To describe quasi-two-dimensional flows it is often tempting to invoke the now well-developed theory of stability of strictly two-dimensional motions (see, for example, Ref. 7). Such attempts, as a rule, have ended in failure, as the authors of such studies themselves point out (see, for example, Refs. 8 and 9). The reason is that friction against the underlying surface cannot be neglected (in the classical theory it is neglected, but it almost always exists in real systems). It plays the decisive role in the development of transcritical rotational flows, coherent structures, and turbulence.

In this review we present the theory of stability and transcritical vortex regimes of quasi-two-dimensional shear flows and its applications to the description of natural and laboratory flows, modeled for the purpose of studying large-scale atmospheric processes. The range of application is limited primarily to the earth's atmosphere; this is connected with the specific scientific interests of the authors. However the theoretical and experimental results presented can be used to describe processes in the atmospheres of other planets, in the ocean, in plasma, and in magnetohydrodynamics of a weakly-conducting liquid, i.e., from this viewpoint they are of importance for physics in general. The material presented should be regarded essentially as an independent branch of hydrodynamics that has not yet been reflected in the physics literature.

1. EQUATIONS OF MOTION, EXTERNAL FRICTION, SIMILARITY CRITERIA

1.1. Thin layers ("shallow water")

We recall that the motion of thin horizontal layers of an ideal incompressible liquid with a free surface in a gravitational field is described by the shallow-water equations (see, for example, Ref. 10)

$$\frac{d\mathbf{v}}{dt} = -\frac{1}{\rho}\nabla(p + \rho g H), \qquad \frac{1}{H}\frac{dH}{dt} + \operatorname{div}\mathbf{v} = 0; \tag{1.1}$$

here $v = v(x, y, t)$ is the two-dimensional vector field of the flow velocity, $H = H(x, y, t)$ is the height of the free surface of the liquid, ρ and g are the density and the acceleration of gravity, and the operator $d/dt = \partial/\partial t + \mathbf{v}\cdot\nabla$. The condition that the layer be thin is $h \ll H_0 \ll L$, where h is the deviation of the height of the free surface from its average value H_0, and L

0038-5670/90/070495-26$01.00

is the characteristic horizontal scale of the flow. This makes it possible to neglect the vertical component of the velocity. The equations (1.1) are identical to the equations of the two-dimensional hydrodynamics of a barotropic[1)] compressible liquid in which H plays the role of the density. It is pertinent to note here that the system (1.1) has a Lagrangian invariant (take the curl of the first equation in Eqs. (1.1) and substitute the result into Eq. (1.2) using the second equation of Eqs. (1.1))

$$I=\frac{\Omega}{H},\quad \frac{dI}{dt}\equiv 0\qquad (\Omega=\mathrm{curl}_z\,\mathbf{v}),\tag{1.2}$$

called the potential vortex.[11-13] In application to the general equations of gas dynamics the expression for the potential vorticity, first found by Ertel,[14,15] assumes the form

$$I=\frac{\Omega\,\mathrm{grad}\,S}{\rho},\tag{1.3}$$

where $\boldsymbol{\Omega}=\mathrm{curl}\,\mathbf{v}$ and S is the specific entropy. Its fundamental importance in theoretical and applied problems in geophysical hydrodynamics is discussed in detail in Refs. 16–19.

The system (1.1) describes, in particular, the propagation of gravity waves on shallow water with the velocity $c=(gH_0)^{1/2}$, which is the analog of the velocity of sound in gas-dynamic systems. For this reason, according to the well-known principle of Ref. 10, to describe slow motions of thin layers of liquid, for which the Mach number $\mathrm{Ma}=v/c\ll 1$, the compressibility can be neglected, setting $H=\mathrm{const}$. The conditions of incompressibility are satisfied, for example, in laboratory experiments[20,21] on the modeling of the shear instability, where the characteristic flow velocities and the thickness of the layer are of the order of 1 cm/s and 1 cm, respectively, and $c\approx 30$ cm/s. To describe flows of this type correctly, however, the viscosity must be taken into account; this creates additional difficulties in the application of the shallow-water theory owing to the impossibility of eliminating the bottom friction, which in its turn destroys the strict two-dimensionality of the flows. In this case, under the assumptions made above, the slow motions of thin layers of liquid, strictly speaking, can be described by equations in which the dependence on the vertical coordinate z enters explicitly:

$$\frac{d\mathbf{v}}{dt}=-\frac{1}{\rho}\nabla p+\nu\Delta\mathbf{v}+\nu\frac{\partial^2\mathbf{v}}{\partial z^2}+\mathbf{F},\tag{1.4}$$

with the boundary conditions on the solid and free surfaces

$$\mathbf{v}|_{z=-H}=0,\quad \left.\frac{\partial\mathbf{v}}{\partial z}\right|_{z=0}=0;\tag{1.5}$$

Here $\Delta=\partial^2/\partial\chi^2+\partial^2/\partial y^2$, ν is the kinematic viscosity, and $\mathbf{F}$ is the external force field. The vertical coordinate is measured from the free surface.

The system (1.4) and (1.5) can be written, after it has been made dimensionless with the help of the characteristic horizontal scales of length L and velocity U of the flow under study, in the form

$$\mathbf{N}(\mathbf{v})\equiv\frac{d\mathbf{v}}{dt}+\frac{1}{\rho}\nabla p-\frac{1}{\mathrm{Re}}\Delta\mathbf{v}-\mathbf{F}=\frac{1}{\mathrm{Re}}\frac{\partial^2\mathbf{v}}{\partial z^2},$$
$$\mathrm{div}\,\mathbf{v}=0,\quad \mathbf{v}|_{z=-h}=0,\ \left.\frac{\partial\mathbf{v}}{\partial z}\right|_{z=0}=0,\tag{1.6}$$

where $\mathrm{Re}=UL/\nu$ is the Reynolds number and $1\gg h=H/L$ is a small parameter. We do not introduce new notation for the dimensionless variables.

We denote $\mathbf{v}_0(x,y,t)=\mathbf{v}|_{z=0}$ the velocity field of the flow on the free top surface of the liquid. Expanding $\mathbf{N}(\mathbf{v})$ in powers of z around $z=0$ and integrating the first equality in Eq. (1.6) twice over z taking into account the boundary conditions, it is easy to obtain the leading term in the expansion of $\mathbf{N}(\mathbf{v}_0)$ in powers of the parameter h:

$$\mathbf{N}(\mathbf{v}_0)=-\frac{2}{\mathrm{Re}\,h^2}\mathbf{v}_0+O(h^2).$$

From here it follows that the last equality is satisfied with accuracy up to terms $O(h^2)$, if the dimensional velocity field on the free surface $\mathbf{u}=+U\mathbf{v}_0$ satisfies the equations

$$\frac{\partial\mathbf{u}}{\partial t}+(\mathbf{u}\nabla)\mathbf{u}=-\frac{1}{\rho}\nabla p+\nu\Delta\mathbf{u}-\lambda_R\mathbf{u}+\mathbf{F},\tag{1.7}$$

$$\mathrm{div}\,\mathbf{u}=0\quad\left(\lambda_R=\frac{2\nu}{H^2}\right).\tag{1.8}$$

The system (1.7) and (1.8) is called the equations of hydrodynamics with Rayleigh friction $\mathbf{f}_R=-\lambda_R\mathbf{u}$. The paradox of this situation is that in spite of the fact that these equations are applicable in a seemingly narrow region they describe a wide range of hydrodynamic phenomena of practical interest, including large-scale processes in the ocean and the atmospheres of rotating planets. The determining physical parameter in them is the coefficient of Rayleigh friction λ_R, the expression for which is not always the same as in Eq. (1.8) and depends on the physics of the hydrodynamic system under study.

1.2. The "shallow water" approximation for a rotating liquid and in magnetohydrodynamics

1. To describe the global processes involved in the general circulation of the earth's ocean and the atmospheres of rotating planets flows for which the Rossby-Kibel number is small $\varepsilon=U/2\Omega_0L\ll 1$; are of greatest interest; here Ω_0 is the angular rotational velocity of the system as a whole and U and L, as previously, are the characteristic velocity and geometric scale of the flow. Flows of this type are in so-called quasigeostrophic equilibrium when the Coriolis force is approximately (with accuracy up to terms of the order of ε^2) balanced by the pressure gradient

$$2\,[\boldsymbol{\Omega}_0\mathbf{v}]\approx-\frac{1}{\rho}\nabla p.\tag{1.9}$$

The quasigeostrophic equilibrium, which was well known to meterorologists back in the last century, is a stable state of global motions. Any local breakdown of this state results in, as shown in Refs. 12 and 22, the emission of acoustic and gravity waves, as a result of which the equilibrium is restored owing to the adjustment of the pressure field to the new wind field.

The relation (1.9) means, in particular, that mass transfer in the atmosphere occurs, at first glance contrary to common sense, not across, but rather along isobars. It is precisely for this reason that air masses in the vicinity of a center of low (high) pressure rotate around this center along spirals converging into it (diverging from it), thereby forming a large-scale vortex–cyclone (anticyclone). The Taylor-Proudman theorem (see, for example, Ref. 13) according to which the equality

$$(\boldsymbol{\Omega}_0\nabla)\,\mathbf{v}\approx 0.\tag{1.10}$$

holds with the same accuracy, follows directly from the relation (1.9) (take the curl of the relation (1.9)). This means that there is virtually no mass transfer anywhere in the direction of rotation of the axis owing to the impermeability of the walls bounding the liquid. This in its turn gives rise to quasistatic equilibrium

$$\frac{\partial p}{\partial z} + g\rho \approx 0, \qquad (1.11)$$

where z is the coordinate in the direction of the axis of rotation of the system as a whole.

The indicated fundamental properties of global geophysical flows make it possible to simplify substantially the starting hydrodynamical equations. We shall illustrate this for the example of a layer of nonviscous incompressible liquid of variable depth with a free surface and rotating around a vertical axis (Fig. 1). Let the relief of the bottom boundary of the layer by given by a function $z = h_1(y)$ of one of the horizontal coordinates. We denote by $h_0 = h_0(x, y, t)$ the deviation of the free surface from the average depth of the layer H_0, so that the depth of the layer is equal to $H = H_0 + h_0(x, y, t) - h_1(y)$. In application to such a system the Taylor-Proudman theorem means that the vertical currents can be neglected, and according to Eq. (1.11) $p = \rho g(H - z)$, if z is measured from the bottom boundary of the layer. The conditions (1.9) of the geostrophic equilibrium assume the form

$$u = -\frac{\partial \Psi}{\partial y}, \quad v = \frac{\partial \Psi}{\partial x}, \quad \Psi = \frac{g}{f} h_0, \quad f = 2\Omega_0 \qquad (1.12)$$

(Ψ is the two-dimensional stream function). The smallness of the Rossby-Kibel number $\varepsilon \ll 1$ implies[13] that the ratio $h_0/H_0 \sim \varepsilon L^2/L_0^2$, is small, if L is not too much greater than $L_0 = (gH_0)^{1/2}/f$—the Obukhov-Rossby scale, which determines the characteristic horizontal size of global vortex formations. We shall now use the theorem of conservation of the potential vorticity (1.2), first we transform to a rotating coordinate system. Then the expression for the potential vorticity, after expanding in the parameter ε, can be written in the form

$$I = \frac{\omega_z + f}{H} = \frac{1}{H_0}\left(\nabla\Psi - L_0^{-2}\Psi + \frac{f}{H_0} h_1\right) + O(\varepsilon^2), \qquad (1.13)$$

where $\omega_z = \Delta\Psi$ is the relative vorticity of the rotating liquid. From the conservation of the potential vorticity $dI/dt = 0$ we obtain the well-known Obukhov-Charney equation:[12,22,23]

$$\frac{\partial}{\partial t}(\Delta\Psi - L_0^{-2}\Psi) + [\Psi, \Delta\Psi] + \beta\frac{\partial \Psi}{\partial x} = 0, \qquad (1.14)$$

$$\beta = \frac{df}{dy} + \frac{f}{H_0}\frac{dh_1}{dy} \qquad (1.15)$$

(in the presence of systematic curvature of the free surface owing to the effect of centrifugal forces an additional term analogous to the second term in Eq. (1.15) must be included here). This equation forms the basis for dynamical meterology and, which is no less interesting from the viewpoint of physical applications, it describes drift waves in a plasma, if the parameters in it are given a different physical interpretation. This is discussed in greater detail in Ref. 24.

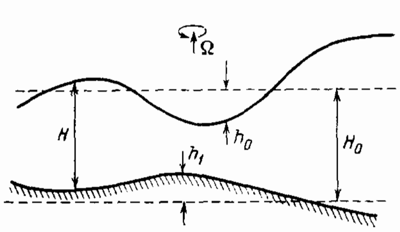

FIG. 1. Schematic diagram of a layer of liquid of variable depth and rotating with the frequency Ω_0.

We stress that for the model under study the Coriolis parameter $f = 2\Omega_0$ is constant, and the so-called β-effect, associated with the presence of the additional linear term on the left side of Eq. (1.14), is obtained here obtained here owing to orography ($dh_1/dy \neq 0$). For the earth's ocean and atmosphere the parameter $f = 2\Omega_0 \sin\varphi$ is two times the earth's angular rotational velocity projected on the normal to the earth's surface and depends on the latitude φ. In this case the coordinates x and y are measured along the longitude and latitude eastward and northward, respectively. The quantity H_0 must be interpreted as the height of a hypothetically uniform atmosphere, whose value is determined from the condition $c^2 = p_0/\rho_0 = gH_0$, where p_0, ρ_0, and c are the pressure, density, and velocity of sound at the ground near the earth's surface ($H_0 \approx 8$ km).

2. The relations (1.9)–(1.11), used in the derivation of the Obukhov-Charney equation, serve as a unique filter[22,25–27] that makes it possible to eliminate from the analysis fast acoustic and gravity waves, which have virtually no effect on the development of global processes, but make it much more difficult to go "big game hunting." The situation with slow waves of a planetary scale is different. The existence of such waves is easiest to illustrate for the β-plane model, when the parameter β, appearing in Eq. (1.14), is assumed to be constant and independent of the latitude. Such a model is often employed to describe oceanic and atmospheric motions at middle latitudes.[13,27] By direct substitution into Eq. (1.14) it is easy to verify that the function

$$\Psi = A\cos(kx + ly - \omega t) \qquad (A = \text{const}) \qquad (1.16)$$

is the exact solution of the Obukhov-Charney equations, describing dispersing waves propagating westward with the phase velocity.

$$c_R = \frac{\omega}{k} = -\beta(k^2 + l^2 - L_0^2)^{-1}. \qquad (1.17)$$

The wave solutions with this dispersion relation are called Rossby waves and sometimes, in application to a spherical earth, Rossby-Gurvits waves (in this case they are expressed in terms of spherical functions; see, for example, Ref. 15). Rossby waves are an important element of the general circulation of the ocean and the atmosphere. They have a significant effect on the characteristics of macroturbulence[28,29] and the instability of global flows. In particular, the resonance interaction of Rossby waves in layered media results in, under certain conditions, an interesting and as yet inadequately studied phenomenon of explosive instability,[30,31] which the linear theory does not pick up. The so-called Rossby solitons, which are not covered by Eq. (1.14), but which play a significant role in cyclogenesis in the ocean and, possibly, in the atmospheres of large planets (when the radius of the planet R is much larger than L_0), occupy a special place in the family of Rossby waves. The review of Ref. 5 is devoted to this question. In particular, in Ref. 5 the methods and results of laboratory modeling of such vortex formations are discussed in detail and compared with natural observations.

The Obukhov-Rossby scale serves as a natural "divide" between Rossby solitons and the waves and vortex structures studied here. The point is that formally, according to the dispersion relation (1.17), the superlong-wavelength waves with wavelength $C_{R\,max} = \beta L_0^2 = cL_0/R$ have the maximum velocity of propagation $L = 2\pi/K \gg L_0$ ($K = (k^2 + l^2)^{1/2} \to 0$) (under terrestrial conditions $L_0 \approx 2000$–3000 km). In addition, $c_{R\,max}$ is comparable to the velocity of sound c. For such velocities and scales Eq. (1.14), still applicable in the vicinity of L_0, no longer works, since the leading term in the expansion (1.13) does not contain terms quadratic in Ψ, which in this case are no longer small. Including these terms results in the appearance in Eq. (1.14) of an additional nonlinearity of the type $(\Psi^2)_x$ ("scalar" nonlinearity in the terminology of Ref. 5), associated not with advection of the velocity ($[\Delta\Psi,\Psi]$) but rather with the rise of the free surface of the liquid. This nonlinearity, as shown in Refs. 32 and 33, is capable of compensating the dispersing influence of the β effect on a wave packet, as a result of which solitary anticyclonic vortices—Rossby wave—can form in the system (in cyclonic vortices the compensation of dispersion by the nonlinearity is impossible, as a result of which there arises the significant cyclonic-anticyclonic asymmetry observed on these scales[5,6]).

From the viewpoint of the problems studied below, this limit of the region of applicability of the equations of dynamic meterology is not fundamental, but these equations make it possible to eliminate the additional technical difficulties in formulating an experiment and in the theory.

3. Global geophysical flows develop, as a rule, under the conditions of rapid rotation, when the Ekman number is small $E = \nu/\Omega_0 H^2 \ll 1$. In this case the transverse circulation of liquid is concentrated in relatively thin Ekman (and, in the presence of vertical walls or other sharp nonuniformities, also in the Stewartson) boundary layers,[34–36] where kinetic energy is mainly dissipated. Thus in the earth's atmosphere up to 70% of the dissipation of kinetic energy occurs in the Ekman planetary boundary layer. For this reason, if one is talking about short development times for motions outside the boundary layers (in the "free" atmosphere) the Obukhov-Charney equation can be used, as this is done, for example, in short-range weather forecasting (one to two days). In the opposite case viscosity must be taken into account.

We recall that the Ekman layer is a unique pump, pumping liquid into or out of the free atmosphere at a rate proportional to the vorticity at its outer boundary:

$$w_E = -\delta_E \xi, \quad \delta_E = \left(\frac{\nu}{f}\right)^{1/2}, \tag{1.18}$$

where δ_E is the effective thickness of the Ekman layer and $\xi = \mathrm{curl}_z \mathbf{v}$.

A striking illustration of the operating principle of the "Ekman pump" is Karman's problem of the motion of a liquid in the vicinity of a rotating flat disk, the exact solution of which is presented in many hydrodynamic texts (see, for example, Ref. 10).

Using the relations (1.18) the equations of two-dimensional motions and conservation of mass of the free atmosphere assume the form

$$\frac{\partial u}{\partial t} + u\frac{\partial u}{\partial x} + v\frac{\partial u}{\partial y} - fv = -\frac{g}{\rho}\frac{\partial \rho H}{\partial x} + \nu\Delta u, \tag{1.19}$$

$$\frac{\partial v}{\partial t} + u\frac{\partial v}{\partial x} + v\frac{\partial v}{\partial y} + fu = -\frac{g}{\rho}\frac{\partial \rho H}{\partial y} + \nu\Delta v,$$
$$\frac{d\rho(H-\delta_E)}{dt} + \rho(H-\delta_E)\left(\frac{\partial u}{\partial x} + \frac{\partial v}{\partial y}\right) = \rho w_E; \tag{1.20}$$

Here the density $\rho = \rho(x, y, t)$ is not assumed to be constant, in order to show explicitly in what follows how external inflows of heat create vorticity in the medium. In this case the system (1.19) and (1.20) must be supplemented by the heat transfer equation and the equation of state, for which the Boussinesq approximation can be used[37]

$$\rho' = \alpha\rho_0 T', \quad \frac{dT'}{dt} = \frac{Q}{c_n}; \tag{1.21}$$

here ρ' and T' are the deviations of the density and temperature from their average values ρ_1 and T_1, α is the thermal coefficient of volume expansion, c_p is the specific heat capacity of the liquid at constant pressure, and Q is the inflow of heat to a unit mass.

From Eqs. (1.19) and (1.20) it follows that the equation of conservation of the potential vorticity (1.2) is now replaced by the equation of transformation of the potential vorticity (the equation of transformation of the potential vorticity was derived in its most general form in Refs. 22 and 38):

$$\frac{d}{dt}\frac{\xi + f}{\rho(H-\delta_E)} = \frac{\nu}{\rho(H-\delta_E)}\Delta\xi + \frac{\xi + f}{\rho(H-\delta_E)^2} w_E. \tag{1.22}$$

Applying to Eq. (1.22), using Eq. (1.21), the same procedure as in the derivation of the Obukhov-Charney equation from the theory of conservation of the potential vorticity, we obtain the following equation describing two-dimensional geophysical flows with Ekman friction $\mathbf{f}_E = -\lambda_E \mathbf{u}$:[39]

$$\frac{\partial}{\partial t}(\Delta\Psi - L_0^{-2}\Psi) + [\Delta\Psi, \Psi] + \beta\frac{\partial\psi}{\partial x} = \nu\Delta^2\Psi - \lambda_E\Delta\Psi + q, \tag{1.23}$$

$$\lambda_E = \frac{\nu}{H_S^2}, \quad q = -\frac{f\alpha Q}{c_p}, \tag{1.24}$$

where, as before, $\Psi = -gh/f$, $u = \partial\Psi/\partial y$, $v = -\partial\Psi/\partial x$, and $H_s = (H_0\delta_E)^{1/2} = H_0^{1/2}\nu^{1/4}f^{-1/4}$ is the thickness of the outer Proudman-Stewartson layer.[34,35]

The equation (1.23) will be used below as the main mathematical tool for the theoretical investigation of the stability and vortex structures of quasi-two-dimensional shear flows. In this connection it is useful to make immediately several remarks that are important from the viewpoint of the interpretation and comparison of laboratory and natural hydrodynamic objects.

First of all, from the mathematical viewpoint the Rayleigh and Ekman friction enter in the same manner in the equation of motion of thin layers of liquid (1.7) and global geophysical flows (1.23). They differ only by the expressions for the coefficients of friction (1.8) and (1.24), from which it follows that in the latter case the measure of effectiveness of the external friction is not the entire height of the layer H_0, but rather the quantity H_S which we shall discuss in our analysis of the vertical structure of quasi-two-dimensional flows. We note only that H_S is the minimum possible scale of the horizontal nonuniformity of a geophysical flow. If the width of the front or the shear of opposite flows significantly exceeds H_S, then the vertical velocities are insignificant. For this reason the criterion of two-dimensionality of geophysical flows is the relation $L \gg H_S$ and not $L \gg H_0$ (which is a much stronger criterion).

Second, it is obvious from the expression (1.24) for q that external inflows of heat are a direct (and not mediated through the temperature field) source of vorticity for a compressible rotating liquid. Under laboratory conditions this makes it possible to replace the heating with a mechanical or some other "drive" that generates a flow with the required profile.

Third, we note that the equations (1.23) can be used to describe a magnetized weakly ionized plasma, where the magnetic field provides the two-dimensionality and the friction against the neutral component gives the Rayleigh term $-\lambda \mathbf{v}$.

Fourth, it is easy to show (see also Refs. 40 and 41) that the equations (1.23) also describe quasi-two-dimensional magnetohydrodynamic flows of a weakly conducting liquid located in a transverse constant magnetic field **B**. Under the assumption of small magnetic Reynolds numbers $\mathrm{Re}_m = UL/\nu_m$ $\nu_m = c_0^2/4\pi\sigma$, where σ is the electric conductivity and c_0 is the velocity of light in a vacuum) and large Hartmann numbers[42] $G = H_0/\delta_G$ $(\delta_G = c_0 B^{-1}(\rho\nu/\sigma)^{1/2})$ the coefficient of bottom friction is equal to $\lambda_G = \nu/H_G^2$, where $H_G = (H_0\delta_G)^{1/2}$. Thus in this case the thickness of the Hartmann boundary layer[42] δ_G is the analog of the thickness of the Ekman layer, while the magnetic field acts analogously to the Coriolis forces.

Finally, in the last few years the Obukhov–Charney equation has found application in astrophysics in connection with the description of the dynamics of galactic disks. In this case, as was pointed out by M. V. Nezlin, it is also necessary to take into account the external friction, which could be caused by the interaction of stars with the interstellar gas.

1.3 Similarity criteria and the possibilities of laboratory modeling

In applying the equation of quasi-two-dimensional flows (1.23) to the description of natural systems, such as the earth's atmosphere and ocean, certain precautions must be taken. First of all, we note an important limitation, caused by the fact that baroclinic effects were neglected in the derivation of Eq. (1.23). From the energy viewpoint baroclinic effects are connected with the transformation of the so-called available potential energy,[13,43] accumulated in a nonuniformly heated liquid owing to buoyancy forces, into the kinetic energy of vertical convective cells, which, in its turn, is transformed into the kinetic energy of horizontal flows owing to the deflecting action of the Coriolis forces. Buoyancy forces appear when the isobaric and isothermal surfaces, the angle between which is a local measure of the excess potential energy, do not coincide. Because of this a convective or, as they say in meterology, baroclinic instability, generated by the nonlinear interaction of the velocity and temperature fields (the advection of the temperature $(\mathbf{v}\cdot\nabla)T$), can develop in the system. The main characteristic of the convective instability of global geophysical flows is their vertical velocity profile, and in addition the vertical gradient of the velocity is proportional to the horizontal gradient of the temperature (the so-called thermal wind ratio[13,27]). This can be easily derived from the geostrophic wind equation (1.9) by writing it in the Boussinesq approximation $(\rho' = \rho_0\alpha T')$ and differentiating with respect to the vertical coordinate.

Thus natural geophysical flows are generated by both the barotropic (connected with the horizontal shear velocity) and baroclinic (connected with the vertical shear velocity) mechanisms of instability. This is a significant obstacle to the construction of a theory of the general circulation of the atmosphere and the ocean, not to mention the difficulties introduced by the orographic and explosive instability. It is precisely for this reason that it is important to know the contribution of each of the indicated mechanisms to the process of cyclogenesis, especially since under laboratory conditions any of them can be excluded, if it is so desired. Another favorable circumstance for the application of the barotropic model is that baroclinic processes develop more slowly than barotropic processes (for example, the characteristic time for assimilation of solar radiation by the earth's atmosphere is of the order of two weeks), which develop over a characteristic time of the order of several days.

Historically, greater attention was devoted first to the baroclinic instability, and the "nonviscous" theory of the barotropic instability was first increasingly studied only at the beginning of the 1970s in connection with the problem of the predictability of atmospheric motions.[44] The "viscous" theory, which, as will be shown below, fundamentally changes the picture of cyclogenesis processes, remained virtually ignored.

Scaling the length and velocity to their characteristic values L and U, the main equation of the quasi-two-dimensional flows (1.23) can be written in the following dimensionless form:

$$\frac{\partial}{\partial t}(\Delta\Psi - \alpha^2\Psi) + [\Delta\Psi, \Psi] + B\frac{\partial\Psi}{\partial x} = R_\nu^{-1}\Delta^2\Psi - R_\lambda^{-1}\Delta\Psi + F; \tag{1.25}$$

here

$$\alpha^2 = \frac{L^2}{L_0^2}, \quad B = \frac{\beta L^2}{U}, \quad R_\nu = \frac{UL}{\nu}, \tag{1.26}$$

$$R_\lambda = \frac{U}{L\lambda} = \frac{UH_*^2}{L\nu}. \tag{1.27}$$

In what follows we shall call the quantity $H_* = (H_0\delta_*)^{1/2}$ the effective thickness of the quasi-two-dimensional flow, where δ_* is equal to the thickness of the Ekman boundary layer $\delta_E = (\nu/f)^{1/2}$ or the Hartmann layer δ_G and by definition is equal to $(1/2)H_0$ for the standard shallow-water model. This makes it possible to standardize the formula for the coefficient of external friction $\lambda = \nu/H_*^2$. The quantity α^2 is called the parameter of horizontal compressibility (for $\alpha^2 = 0$ the Obukhov-Charney equation (1.14) is identical to the equation of motion of an incompressible two-dimensional film in the β plane or on a sphere), B characterizes the strength of the β effect, R_ν is the standard Reynolds number, and it is convenient to interpret R_λ as the Reynolds number with respect to the external friction,[45,46] which, it should be noted, is made up of a combination of all dimensional characteristics (H_0, ν, δ_*, L, U) of the quasi-two-dimensional flow. We also note that the a priori assumption

TABLE I. The values of the parameters of the earth's atmosphere at the latitude $\Phi_0 = 45°$.

H_0, км	L_0, км	f, с$^{-1}$	δ_E, км	H_*, km	β, с$^{-1}$m^{-1}	ν, cm^2/s	U, m/s	M	E
10	$3\cdot10^3$	10^{-4}	0.5	2.2	$1.6\cdot10^{-11}$	25	10	0.03	$2.5\cdot10^{-3}$

that the Mach number ($M = U/(gH_0)^{1/2}$), the Rossby number ($\varepsilon = U/fL$), and the Ekman number $E = \nu/fH_0^2 = \delta_E^2/H_0^2$) are small ensures that the system is self-similar relative to these parameters, which do not appear in Eq. (1.25).

The complete investigation of the solutions of Eq. (1.25), described by the four outer parameters, is a difficult to grasp problem. For this reason, to choose a concrete direction of theoretical analysis and to formulate laboratory experiments it is useful to have estimates of the values of the indicated similarity criteria for real flows. As an example, Tables I and II give the values of the dimensional parameters of the earth's atmosphere and the similarity criteria for different scales of atmospheric motions. It should be noted that in estimating the quantities indicated above ν was taken to be the coefficient of small-scale turbulence, which has a dissipative effect on flow with scales of the order of hundreds and thousands of kilometers. From the tables one can see, in particular, that the conditions for M, ε, and E to be small are satisfied well everywhere except for the neighborhood $L = 100\ km$ where $\varepsilon \sim 1$. An appreciable effect of the parameters α^2 and B can be expected only for scales of the order of 1000 km and larger. Finally, the characteristic feature of large-scale atmospheric flows is that for them $R_\nu \gg R_\lambda$.

In laboratory experiments[21] with "shallow water" the thickness H_0 of the layer of liquid, for which water or its salt solutions ($\nu \approx 0.01$ cm^2/s) is used, is usually of the order of 1 cm, the characteristic horizontal scale of the flow $L \approx 3$–5 cm, and the characteristic flow velocity $U \approx 0.1$–2 cm/s. In experiments with a rotating liquid[47–49] $\Omega_0 \sim 1\ s^{-1}$ (~ 10 rpm), $U \approx 0.3$–3 cm/s, and $L \approx 2$–10 cm. It is easy to verify that in experiments of this type the conditions for M, ε, and E to be small are also satisfied. The value of the parameter B need not be compared, since under laboratory conditions this parameter can be easily controlled with the help of the bottom relief (see the formula (1.15)). The values of R_λ range from several tenths to tens, as in the atmosphere while $R_\nu \sim 10$–10^3, i.e., it is two to four orders of magnitude lower than in the atmosphere. Such a significant difference between the laboratory values of R_ν and the values of R_ν found in nature casts doubt on the possibility of modeling atmospheric processes under laboratory conditions and has often served as a serious argument against the use of the results of laboratory studies to explain the processes occurring in the general circulation of the atmosphere. We note that the characteristic laboratory value of the Obukhov-Rossby scale $L_0 = (gH_0)^{1/2}/f \sim 50$ cm, which also creates definite difficulties in modeling flows for which $\alpha^2 \sim 1$. For this, either the rate of rotation must be significantly increased[5,6] ($L_0 \sim 5$ cm with 100 rpm) or quite large cylindrical vessels not less than 1 m in diameter must be used. Thus the questions connected with laboratory modeling of large-scale atmospheric flows require additional theoretical analysis; this in particular, will be discussed below.

2. THE LINEAR THEORY OF STABILITY

It has been well known[7,50] since the last century that one of the main reasons for hydrodynamic instability is shear of the flow velocity, i.e., the existence of inflection points in the profile of the flow velocity. For example, in the case of a tangential discontinuity (Fig. 2) the motion of an ideal liquid is exponentially unstable with respect to any wave-like disturbance, whose increment depends on the wave number $k = 2\pi/\lambda$ (λ is the wavelength) and is equal to $\gamma = kU$ (U is the magnitude of the velocity shear). Figure 3 shows the dependence $\gamma = \gamma(k)$ for a "diffuse discontinuity" of width D. One can see from Fig. 3 that eliminating the velocity discontinuity stabilizes the flow with respect to small-scale perturbations. These examples illustrate not only the fact of instability of shear flows itself, but they also show that great care must be exercised in idealizing the profile of a real flow, on which the characteristics of stability strongly depend. In any case, the presence of viscosity imposes certain requirements on the smoothness of the profile of the flow velocity; neglecting them can lead to incorrect results.

The viscous and nonviscous theory of the stability of strictly two-dimensional shear flows is now well developed. But, as mentioned above, it is not directly applicable for describing quasi-two-dimensional flows. The situation, however, changes, if the results of the theory are given a different hydrodynamic meaning. In this connection we shall now briefly discuss the basic results of the classical theory.

2.1. The results of the classical theory of stability of two-dimensional shear flows

The classical problem of the theory of stability for Eq. (1.23) is formulated as follows. Let the "force" q depend only on the transverse coordinate y and be directed along x.

TABLE II. The values of the similarity criteria for different scales of atmospheric motions.

L, km	100	300	500	1000	3000
$\varepsilon = U/fL$	1	0.3	0.2	0.1	0.03
α^2	0.001	0.01	0.03	0.1	1
B	$1.6\cdot10^{-2}$	$1.4\cdot10^{-1}$	0.39	1.6	14
R_ν	$4\cdot10^4$	$1.2\cdot10^5$	$2\cdot10^5$	$4\cdot10^5$	$1.2\cdot10^6$
R_λ	20	6.7	4	2	0.7

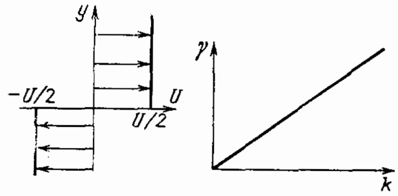

FIG. 2. The velocity profile and the dispersion curve of a tangential discontinuity.

Then Eq. (1.23) has a steady-state solution, describing the "main flow" $\Psi_0(y)$ with velocity $U(y)$, directed along the x axis and depending only on y. The problem is to study the stability of this solution with respect to small perturbations.

In the absence of the β effect, external friction, and "two-dimensional compressibility" ($\beta = 0$, $\lambda = 0$, $L_0^{-1} = 0$) the linear problem of stability reduces to the problem of finding the eigenvalues of the Orr-Sommerfeld equation[7,50]

$$[U - (c_r + ic_i)](\varphi'' - \alpha\varphi^2) - U''\varphi = \frac{i}{\alpha R_\nu}(\varphi^{IV} - 2\alpha^2\varphi'' + \alpha^4\varphi) \tag{2.1}$$

with the boundary conditions for attachment on the side boundaries $\alpha\varphi = \psi' = 0$ at $y = y_1$ and y_2; here φ is the dimensionless amplitude of a harmonic disturbance with the stream function

$$\psi = \varphi(y)\exp[i\alpha(x - ct)], \quad c = c_r + ic_i, \tag{2.2}$$

α is the dimensionless wave number and $\gamma = ac_i$ is an increment that takes on a positive value for unstable modes. The theorem of Squires,[7,50] according to which the most dangerous disturbances are the disturbances lying in the plane of the main flow, makes it possible to restrict the problem to two dimensions. The purpose of the linear theory of stability is to obtain the dispersion dependence $\gamma = \gamma(\alpha)$ of the growth increment of the disturbance on the wave number.

Most results of the linear theory pertain to the particular case $\nu = 0$—the Rayleigh equation

$$[U - (c_r + ic_i)](\varphi'' - \alpha^2\varphi) - U''\varphi = 0 \tag{2.3}$$

with the impenetrability boundary conditions $\alpha\varphi = 0$ at $y = y_1$ and y_2. Rayleigh's equation, in contradistinction to Eq. (2.1), is invariant relative to complex conjugation with accuracy up to a change of the sign of c_i. For this reason the existence of a solution with negative c_i implies the existence of a complex conjugate solution with $c_i > 0$. Therefore in the nonviscous theory any $c_i \neq 0$ means instability—a property which the solutions of the Orr-Sommerfeld equation do not have. In this connection it is appropriate to mention the important result of Lin and Wasov,[50,51] according to which only the growing ($c_i > 0$) solutions of Rayleigh's equation are limits of the solutions of Eq. (2.1) as $\nu \to 0$. Some typical dispersion curves, obtained by different authors, are presented in Fig. 4.

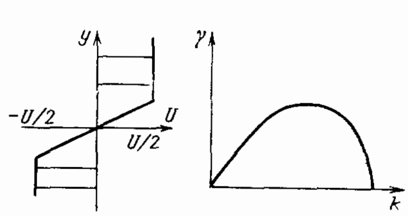

FIG. 3. Same as in Fig. 2 for a "smeared discontinuity."

The curve (l) in Fig. 4 corresponds to a piecewise-linear profile

$$\begin{aligned} U &= y\,|y|^{-1} \quad \text{for } |y| \geqslant 1, \\ &= y \qquad\quad \text{for } |y| \leqslant 1 \end{aligned} \tag{2.4}$$

and is described by a formula first derived by Rayleigh (see, for example, Ref. 52)

$$\gamma = \frac{1}{2}[e^{-4\alpha} - (1 - 2\alpha)^2]^{1/2}. \tag{2.5}$$

The curve (s) for the sinusoidal profile $U = \sin y$ is given by the approximate formula

$$\gamma = \alpha\left(\frac{1}{2}\,\frac{1-\alpha^2}{1+\alpha^2}\right)^{1/2}, \tag{2.6}$$

which can be easily derived from the results presented in Ref. 53. The dispersion curves (e) and (t) for the profiles $U = \mathrm{erf}(y)$ and $U = \tanh y$ were obtained by numerical integration.[54–56] We note that except in rare cases Rayleigh's equation cannot be solved exactly analytically. The asymptotic expressions for the dispersion relations and eigenfunctions in neighborhoods of the neutral points $\alpha = 0$ and $\alpha = \alpha_s \neq 0$ (where $\gamma = 0$) for different velocity profiles can be found in Refs. 50, 55, and 7.

Figure 5a shows the dispersion curves obtained in Ref. 54 (see also Ref. 8) for the viscous problem for $U = \tanh y$ by numerical integration with different values of the Reynolds number R_ν. Figure 6 shows the neutral curves $R_\nu^*(\alpha)$ for the same profile and for $U = \sin y$ according to the formula[53]

$$R_\nu^* = \sqrt{2}\,\frac{1+\alpha^2}{(1-\alpha^2)^{1/2}}. \tag{2.7}$$

It is easy to see that, as opposed to the sinusoidal profile for which instability starts at $R_\nu > \sqrt{2}$, the profiles (e), (l), and (t) are always unstable, since in a neighborhood of $\alpha = 0$ the long-wavelength modes see the flow as a Helmholtz flow $U = y/|y|$. For the same reason near $\alpha = 0$ the behavior of the dispersion curves in Fig. 1 is virtually independent of the profile of the main flow. In addition, for profiles of the same type (e), (l), and (t) the maximum values of γ are virtually

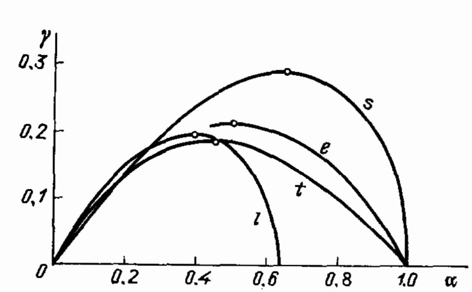

FIG. 4. Dispersion curves $\gamma(\alpha)$ for $U = \sin y$ (curve 2), erf y (curve e), tanh y (curve t), and a piecewise-linear profile (curve l) in the nonviscous case.[53,55,56]

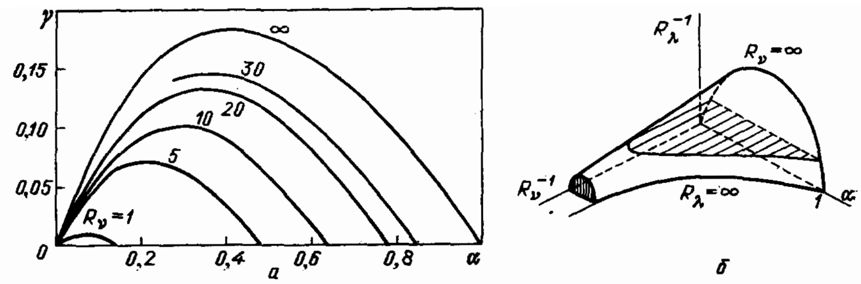

FIG. 5. a) The dispersion curve $\gamma(\alpha,R_\nu)$ for $U=\tanh y$.[54] b) Surface of neutral stability $F(\alpha,R_\lambda,R_\nu)=0$ for $U=\tanh y$.[45]

identical. We note finally that above some critical Reynolds number it is the long-wavelength modes $\alpha\to 0$ that are excited first.

2.2 The role of external friction

The importance of taking external friction into account in concrete problems has been pointed out repeatedly in the hydrodynamic literature. Thus in Ref. 9 taking dissipation in the Ekman layer into account made it possible to match the theoretical and experimental results for the stability of shear flows of a rotating liquid, and in Refs. 57–59 this was done for flows with a sinusoidal velocity profile in a thin layer of liquid. We call attention especially to Ref. 60, where a weakly nonlinear theory is actually constructed (see Sec. 4 for a more detailed discussion of this). In the general form, however, the effect of external friction on the linear stability of shear flows was analyzed only in Ref. 45.

Consider, once again, Eq. (1.23) with $\lambda\neq 0$. The simplest estimate shows that the term with λ predominates over the term with ν, if the characteristic horizontal scale of the flow L exceeds the quantity $L_{\min}=(\nu/\lambda)^{1/2}=H_*$ (see Sec. 1.4). But this condition is also the criterion for the flow to be two-dimensional! Hence it can be expected that in quasi-two-dimensional flows the main mechanism of dissipation is external friction and not internal viscosity (in other words, the vertical and not the horizontal diffusion of momentum). Of course, this result must be approached with some care, since, generally speaking, in the region of large gradients it could be dangerous to delete from the equations the term with the highest order derivative ($\nu\Delta^2\Psi$). We shall study the consequences of introducing external friction into the viscous equation (1.23) (as before, setting $\beta=0$, $L_0^{-1}=0$).

It is easy to see that from the viewpoint of the linear theory of stability external friction only reduces the (dimensional) increments of growth of wave disturbances by an amount λ without changing the form of the dispersion curves and the eigenfunctions. Indeed, for perturbations of the form (2.2) the Orr-Sommerfeld equation assumes the form

$$\left[U-\left(c_{r\lambda}+ic_{i\lambda}+\frac{i}{\alpha R_\lambda}\right)\right](\varphi''-\alpha^2\varphi)-U''\varphi$$
$$=\frac{i}{\alpha R_\nu}(\varphi^{\mathrm{IV}}-2\alpha^2\varphi''+\alpha^4\varphi), \tag{2.8}$$

where the real and imaginary parts of the complex quantity c are given an index λ in order to distinguish them from the case $\lambda=0$. This equation is identical to Eq. (2.1) to within the substitution $c_{i\lambda}+(\alpha R_\lambda)^{-1}\to c_i$. Recalling that $F=\alpha c_{i\lambda}$ is the growth increment of the disturbance we find that the dispersion relation for Eq. (2.8) assumes the form $F(\alpha,R_\lambda,R_\nu)\gamma(\alpha,R_\nu)-R_\lambda^{-1}$, where $\gamma=\gamma(\alpha,R_\nu)$ is the dispersion curve of Eq. (2.1). Now the critical curve (the curve of neutral stability) is given by the equality

$$F(\alpha,R_\lambda,R_\nu)\equiv\gamma(\alpha,R_\nu)-R_\lambda^{-1}=0 \tag{2.9}$$

(the increment of instability is equal to the damping decrement determined by the external friction). Thus to study the effect of bottom friction on the stability of shear flows it is sufficient to use the well-known results of the classical theory, which thereby are given a new hydrodynamic interpretation. In particular, the dispersion curves in Figs. 4 and 5a can be regarded only as curves of neutral stability of shear flows taking into account the bottom friction, if R_λ^{-1} instead of γ is plotted along the ordinate axis. However, from this, almost obvious, assertion there follow, after some additional considerations, nontrivial results.

We shall first study two limiting cases of the critical condition (2.9) for the problem (2.8): the limits $R_\lambda\to\infty$ and $R_\nu\to\infty$ (R_λ and R_ν are independent dimensionless parameters). Evidently, $\lim F=\gamma(\alpha,R_\nu)$ as $R_\lambda\to\infty$ and $\lim F=\gamma(\alpha)-R_\lambda^{-1}$ as $R_\nu\to\infty$, where $\gamma=\gamma(\alpha)$ is the dispersion relation of Rayleigh's problem (2.3). The latter equality follows from the above-mentioned result of Lin and

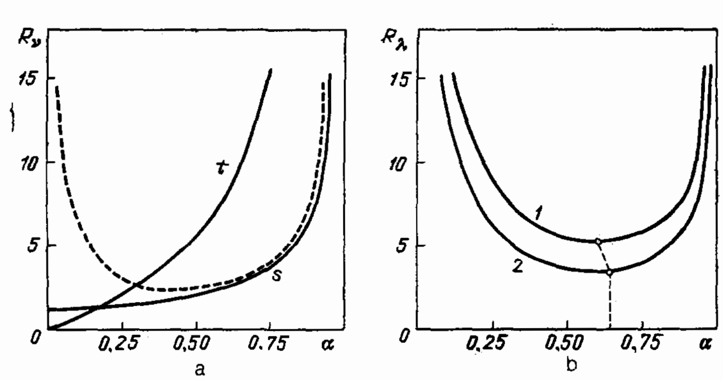

FIG. 6. a) Neutral curves for $U=\sin y$ (curve s) and $\tanh y$ (curve t) without external friction as well as for $U=\sin y$ with $R_\nu/R_\lambda=0.1$ (dashed curve). b) Same for $U=\sin y$ for $R_\nu/R_\lambda=1$ (curve 1) and ∞ (curve 2).

Wasow[50,51] for the positive eigenvalues $\gamma = \alpha c_i$, whose role R_λ^{-1} plays. As one can see by comparing Figs. 4 and 6 taking into account the new interpretation, the neutral curves corresponding to the indicated limiting cases differ fundamentally in their behavior in the neighborhood of $\alpha = 0$ and the position of their minima (maxima). It already essentially follows from here that the external friction gives a new quality to the characteristics of stability of shear flows. The question, however, is whether this new quality is a consequence of passing to the limit in the dispersion relation for the problem (2.8) as $R_\nu \to \infty$ or, conversely, whether the new quality is lost as a consequence of passing to the limit as $R_\lambda \to \infty$. Thus the problem reduces to studying the structural stability of the neutral curves

$$R_\lambda^{-1} = \gamma(\alpha, R_\nu), \qquad R_\nu = R_\nu(\alpha, R_\lambda), \tag{2.10}$$

given by the dispersion relation (2.9) in a neighborhood of the points $R_\nu^{-1} = 0$ and $R_\lambda^{-1} = 0$, respectively, with respect to small changes in their parameters.

In its general formulation this is a very complicated mathematical problem. For this reason we shall confine our attention to heuristic considerations, based on the results of the classical theory and reinforced with a specific example and experimental data. In the case at hand the set of points of neutral stability, determined by the dispersion relation (2.9), forms a unique conical surface in the space of the parameters $(\alpha, R_\lambda^{-1}, R_\nu^{-1})$ shown in Fig. 5b for $U = \tanh y$. It is not difficult to construct the indicated surface by using the data in Fig. 5a taking into account their new interpretation. The other mentioned profiles of shear flows evidently also have analogous surfaces of neutral stability with the only insignificant difference being that for $U = \sin y$ the tip of the cone lies not at infinity but rather on the R_ν^{-1} axis at the point $R_\nu^{-1} = 1/\sqrt{2}$ (see Eq. (2.7)). The horizontal and vertical sections of the neutral surface coincide with the neutral curves (2.10) and, as one can see from Fig. 5b, have a horseshoe shape, with the exception of the single curve in the plane $R_\lambda^{-1} = 0 (\lambda = 0)$, which recedes to infinity or crosses the R_ν^{-1} axis at the point $R_\nu^{-1} = 1/\sqrt{2}$.

Thus from the viewpoint of the new formulation of the problem the classical critical curve is a special curve, structurally unstable with respect to the inclusion of external friction. Conversely, the form of the critical curves taking external friction into account is insensitive to inclusion or exclusion of internal viscosity, i.e., the characteristics of stability do not undergo any qualitative changes as the parameter R_ν is varied. We shall illustrate this for the example of the concrete dispersion relation for $U = \sin y$

$$R_\nu = \left[\frac{2(1+\lambda_0+\alpha^2)(\lambda_0+\alpha^2)(1+\alpha^2)}{\alpha^2(1-\alpha^2)}\right]^{1/2} \qquad \left(\lambda_0 = \frac{R_\nu}{R_\lambda}\right), \tag{2.11}$$

derived in Refs. 57 and 59. One can see that the curve

$$R_\nu(\alpha) \equiv R_\nu(\alpha, 0) = \frac{\sqrt{2}(1+\alpha^2)}{(1-\alpha^2)^{1/2}}$$

is not the uniform (with respect to α) limit of the curve (2.11) as $\lambda_0 \to 0$.

The qualitative change occurring in the neutral curves when external friction is included is manifested, in particular, in the fact that above the threshold of stability the disturbances with finite wave number, corresponding to the maximum neutral curve, and not the long-wavelength modes, as before, are excited first. Finally, based on what we said at the start of this section, it can be asserted that in the case of real quasi-two-dimensional flows with sufficiently large horizontal scales ($L \gg H_*$) the effect of viscosity is in general negligibly small. This means that the transition to instability is determined solely by the value of the Reynolds number with respect to the external friction and the neutral curve $R_\lambda^* = R_\lambda^*(\alpha)$ is found from the dispersion curve for Rayleigh's equation $R_\lambda^* = \gamma(\alpha)^{-1}$. In this case, based on the data of Fig. 4, we can immediately predict the approximate values of the critical Reynolds number $R_\lambda \sim 5$ and the dimensionless wave number $\alpha_0 = \alpha_{0d} L \sim 0.5$ of the disturbance arising after the flow with the shear velocity profile of the type $U = \tanh y$ becomes unstable (the index d denotes a dimensional quantity).

Another important consequence[61] of taking into account external friction is the "vanishing" of the critical layer, since the singular point y_c of the equation of linear stability (2.8), in which $U(y_c) = c_\lambda + i/\alpha R_\lambda$ is displaced into the complex plane (the critical layer is a neighborhood of the point y_c in which the phase velocity of the neutral disturbance with $\lambda = 0$ is equal to the velocity of the flow). As we shall see below, this substantially simplifies the "nonlinear" analysis.

Finally, we note that the self-similarity of the problem with respect to R_ν for large values of R_ν makes it possible to eliminate the question of the correspondence between the laboratory experiments and atmospheric flows and to explain why relatively regular vortex structures are observed in the atmosphere on large scales (Fig. 7). The values of R_ν for the atmosphere are of the order of 10^{12}, if the molecular

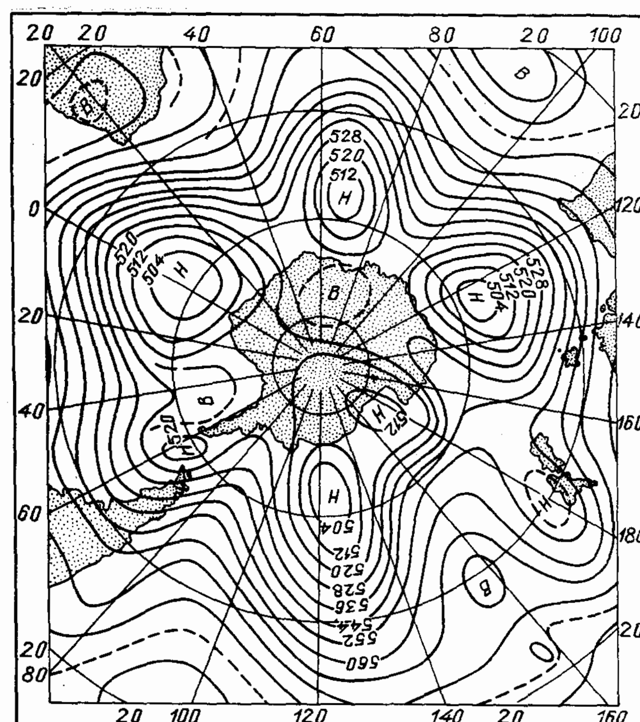

FIG. 7. map of isobars above the South Pole.

kinematic viscosity is used for ν, and of the order of 10^6, if the value of the turbulent viscosity is used. At first glance this means that the atmosphere should be a turbulent "boiling cauldron." Now, when we know that the system is self-similar with respect to R_ν and the determining parameter is R_λ, the supercriticality of large-scale flows should be evaluated with respect to the value of R_λ. One can see from Table 2 that R_λ fluctuates in a neighborhood of the critical value.

Finally it is pertinent to note that the conclusion that the results of the classical theory of strictly two-dimensional flows are structurally unstable is of a more general character. An analogous situation will occur if stratification, a magnetic field, or rotation of the system as a whole affects the liquid instead of the external friction. In particular, the critical curve for nonviscous shear flow of a stratified liquid in the parameter plane (Ri, α) (Ri is Richardson's number, $\mathrm{Ri} = gH\Delta\rho/\rho_0 U^2$, where g is the acceleration of gravity, $\Delta\rho$ is the characteristic difference of the densities in the liquid, H is the characteristic vertical scale, U is the magnitude of the shear, and ρ_0 is the average density), as is well known, has a horseshoe shape with the maximum value Ri = Ri = 1/4, (the theorem of Miles[62,63]). It is easy to understand that the surface of neutral stability for a viscous flow of a stratified liquid in the parameter space (Ri, R_ν^{-1}, α) will also have a form analogous to that in Fig. 5b.

In connection with the analogy mentioned above it is helpful to call attention to a circumstance that is at first glance paradoxical. We recall that in the absence of internal viscosity the critical value R_λ^* for quasi-two-dimensional flows of a homogeneous liquid depends, though weakly, on the form of the profile, while for stratified flows the critical Richardson's number has a universal value, equal to Ri* = 1/4, for any stable provile of stratification. This fact has, however, a simple physical explanation, which, strangely enough, is practically never encountered in the literature.

A stratified liquid can in a certain sense be regarded as the hydrodynamic analog of a mechanical pendulum.[64,65] We shall assume that the state of the pendulum is "stable," if in its motion it does not reach the top position of equilibrium. Then the condition of stability can be formulated in the form of the inequality $2\Pi/K > 1$, where $2\Pi = 2mgh$ is the potential energy of the top position of equilibrium relative to the bottom position of equilibrium, and $K = mv^2/2$ is the kinetic energy of the pendulum at the bottom point. This criterion can also be interpreted as the condition for the conversion of the oscillatory energy of the pendulum into rotational energy, and in application to the liquid as the conversion of wave energy into rational energy.

We shall formally apply the criterion of stability to a particle of liquid located in a stratified shear flow at a distance Δz from some horizontal plane $z = z_0$. Then taking into account the action of the buoyancy force the quantity Π can be written in the form $\Pi = g\Delta z\Delta\rho$ ($\Delta\rho = \rho_0 - \rho(z)$, $\rho_0 = \rho(z_0)$), and in a coordinate system moving with the velocity of the liquid the quantity K at the point $z = z_0$ is equal to approximately $\frac{1}{2}\rho_0\Delta u^2 = \rho_0(u(z_0) - u(z))^2/2$. Passing now to the limit $\Delta z \to 0$ and transferring the twos to the right side of the inequality, we obtain

$$\lim_{\Delta z\to 0}\frac{g\Delta\rho\Delta z}{\rho_0\Delta u^2} = \lim_{\Delta z\to 0}\frac{g\Delta\rho/\Delta z}{\rho_0\,(\Delta l/\Delta z)^2} = \frac{g d\rho/dz}{\rho_0\,(du/dz)^2} \equiv \mathrm{Ri}_l > \frac{1}{4},$$

where Ri_l is the local Richardson number. It is easy to see that an analogous criterion also holds for the global Richardson number, defined above. Thus we have explained the universality of the critical value of Richardson's number and why Ri* is equal to precisely 1/4.

3. LABORATORY EXPERIMENTS

3.1. Methods of laboratory modeling

Experimental investigations of the instability of shear flows have a long history. However a significant part of the papers is devoted to the so-called mixing layers (see, for example, the reviews of Refs. 66 and 67), in which the instability develops downstream. Here we shall study only experiments with a forcing layer that is constant in time. In these experiments the flows are of steady state or (for large supercriticalities) of a self-oscillatory character.

Quasi-two-dimensional flows in such experiments are realized either in thin layers of liquid or in a rotating liquid (we shall term a liquid rotating, if its depth is much greater than the thickness of the Ekman boundary layer), where, according to the Taylor-Proudman theorem, the vertical motions are impeded. As a rule, these experiments are performed in cylindrically symmetric setups. The liquid confined in a cylindrical or annular vessel can be put into motion by relative rotation of the end boundaries, a volume force (for example, Ampere's force), or sources and sinks of mass.

The flow in all cases has some common features. First of all, for low slip velocities, as a rule, it is possible to observe a stable shear layer. As the velocity increases the shear layer becomes unstable, and a regular chain of vortices of the "cat's eye" type arises. Further increase of the velocity results in a decrease of the number of vortices generated by the shear flow and the appearance of self-excited oscillations, and the vortex regimes are no longer unique. However the magnitude of the critical slip velocity and the number of vortices n_0 arising immediately after instability appears are determined uniquely by the external parameters of the flow and can be reproduced. Thus in all experiments primarily the critical parameters—the magnitude of the shear and the

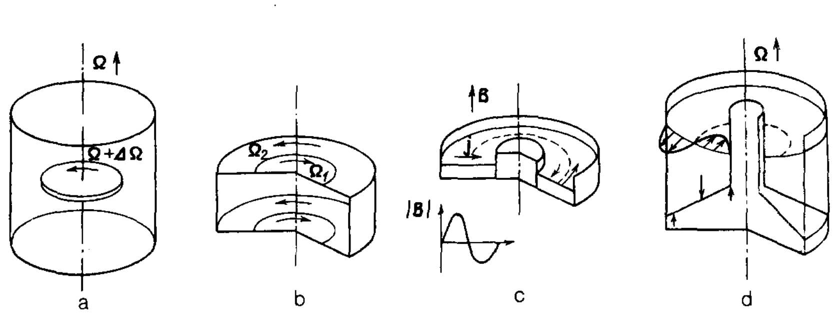

FIG. 8. Diagrams of the basic types of setups used for modeling forced shear flows. a) Ref. 68, b) Refs. 70 and 102; c) MHD method (Refs. 71 and others) (B is the magnetic field, j is the electric current); d) method of sources and sinks (Refs. 21 and others) (the thick arrows mark the position of the sources and sinks).

number of vortices n_0—are measured. In all papers the dependences of the number of vortices (or of the dimensionless wave number obtained from it) on the amplitudes of the shear are also presented.

One of the first experiments was the experiment of Ref. 68 on the investigation of the stability of a vertical shear layer (Stewartson-Proudman layer) in a rotating liquid. The flow was created in a rotating tank by means of slow relative rotation of a disk with a small radius placed in the volume of the liquid (Fig. 8a). In the experiment the rate of rotation of the tank and the radius of the disk were varied.

An analogous apparatus was employed in Ref. 69 with the difference that the thin disk was placed at the bottom of the tank (the construction made it possible to generate both an isolated shear and a jet flow). The angular rotational velocity of the tank was the variable external parameter.

The stability of a shear flow in the narrow gap between two rotating disks was studied in Ref. 70. Each disk consisted of a small disk and a ring rotating with different angular velocities (Fig. 8b). The angular velocities were low, so that the liquid can be regarded as nonrotating. In the experiment the thickness of the layer of liquid and the radius of the shear were measured.

In Refs. 57 and 71–78 the magnetohydrodynamic method was employed to model shear flows in a thin layer of nonrotating liquid (Fig. 8c). It is based on the fact that a weakly conducting liquid placed in a vertical magnetic field starts to move under the action of Ampere's force $F_A \propto \mathbf{j} \times \mathbf{B}$ ($\mathbf{j}$ is the electric current density and $\mathbf{B}$ is the magnetic field) when an electric current is passed through the liquid in the horizontal direction. By varying the form of the magnetic field it is possible to obtain different velocity profiles of the main flow. Flows with a sinusoidal velocity profile in a rectangular cell[57,75,76] (Kolmogorov flow[20,53]) and in an annular channel,[71–74] flows with a narrow zone of shear[77] (of the type $U = \tanh y$), and stream flows[78] have been studied. In the experiments the thickness of the layer of liquid and the width of the shear zone were varied; the width of the shear zone was varied by changing the structure of the magnetic field. It is pertinent to note that in all experiments the value of Hartmann's number was small, so that the thickness of the Hartmann layer was much greater than the depth of the liquid, and the flow did not have a Hartmann profile, but rather a Poiseuille vertical profile of the velocity. The opposite situation was studied in Refs. 40 and 41.

Another group of investigations is devoted to the study of a rotating liquid with a "topographic" β effect, arising owing to the sloping of the bottom of the vessel and/or of the free surface. In Ref. 80 a jet flow was generated by a narrow ring, rotating slowly relative to the vessel. In Refs. 47–49 and 80–82 the method of sources and sinks was used (Fig. 8d). This method is based on the fact that forced pumping of the liquid in the radial direction results in the appearance of azimuthal flow as a result of the deflecting action of the Coriolis force (this is discussed in greater detail below). We note that in Refs. 81 and 82, in contrast to other papers, the flow was turbulent.

Finally, in Refs. 5 and 6 a vessel with a parabolic shape was employed. This made it possible to study the motion of a layer with constant thickness and high rotational velocities, when the scales of the flow exceed the Rossby-Obukhov radius. A shear was created by independent rotation of rings placed on the bottom of the vessel, and the relative velocities exceeded the velocity of gravity waves, i.e., the flows were "supersonic."

In the next subsection we shall describe in detail the results of the experiments of Ref. 77, which were specially formulated in order to investigate the effect of external friction.

3.2. Shear and jet flows in annular channels

The shear flow in the experiments of Ref. 77 was generated by the MHD method. The main piece of equipment is a system of annular magnets or electromagnets, which generates an azimuthally symmetric magnetic field, whose vertical component changes sign in the radial direction. The apparatus and the magnetic field generated by it are described in detail in Refs. 71–73. A circular cell with annular electrodes placed in it is placed on top of an electromagnet. A layer of electrolyte ($CuSO_4$ solution, $\rho = 1.07$ g/cm^3, and $\nu = 0.012$ cm^2/s) is poured into the cell. An electric current (radially directed) from a stabilized source is passed between the electrodes. The liquid is put into azimuthal motion by the action of Ampere's force, and the velocity profile is determined by the profile of the magnetic field and the arrangement of the electrodes.

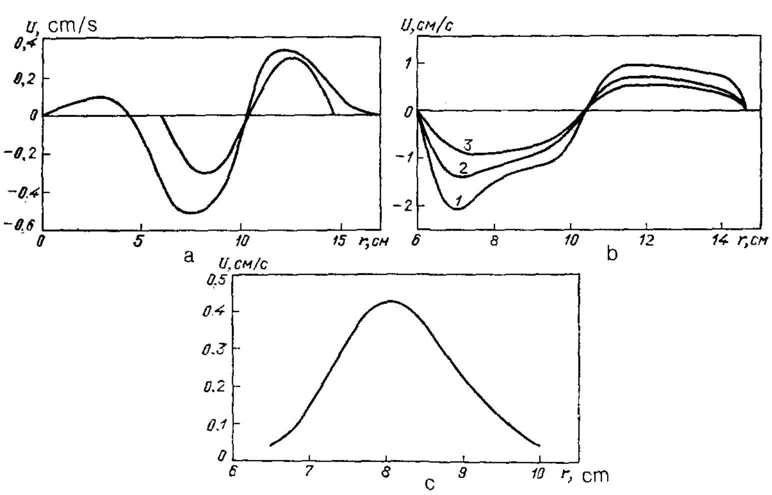

FIG. 9. Experimental profiles of the azimuthal velocity for the critical value of the Reynolds number for flows of the type $U = \sin y$ in an annular channel[73] and with "impedance" side boundaries[74] (a); $U = \tanh y$ (Ref. 77) for $H_0 = 3$ mm (1), 4 mm (2), and 5 mm (3) (b). c) Jet flow.[78]

We point out that depending on the distance to the magnet the radial profile of the vertical component of the magnetic induction changes from almost rectangular (nearby) to nearly sinusoidal (far away). By changing the configuration of the electrodes and the position of the cell it is possible to obtain different profiles of the azimuthal velocity. In the experiments the following profiles were realized: a sinusoidal profile with rigid and impedance (free surface) side boundaries, flow with a narrow zone of shear (of the type $U = \tanh y$), and a jet flow (Fig. 9). The flow was visualized by placing aluminum powder on the surface of the liquid. All measurements of the velocity were performed from track photographs of the particles in the visualizer. In each experiment the magnitude of the magnetic field, the depth of the liquid, and the position of the cell were held constant, and only the strength of the current was changed. This makes it possible to assume that the profile of the force acting on the liquid is constant and that the amplitude of the force is related uniquely with the current strength. This amplitude is characterized by the dimensionless Reynolds number "along the head"

$$R_f = \frac{I B_0 L_B^2}{2\pi\rho c H_0 \nu^2}, \tag{3.1}$$

where I is the current strength, B_0 is characteristic magnitude of the magnetic induction, ρ is the density of the liquid, H_0 is the depth of the liquid, ν is the viscosity, c is the velocity of light (in vacuum), and L_B is the scale of variation of the magnetic field.[72,73] As we have already mentioned, in these experiments Hartmann's numbers were small, i.e., $\delta_G \gg H_0$, so that in this case $\lambda = 2\nu/H_0^2$.

For small values of the Reynolds' number the fluid flow is azimuthally symmetric. The streamlines are concentric circles. Above the critical value R_f^* the azimuthal symmetry is destroyed, and an azimuthally periodic rotational or wavy (jet) flow with symmetry index n_0, which depends on the geometric parameters (Fig. 10), arises. For shear flows the centers of the vortices lie on the neutral line of the magnetic field ($B_z = 0$), where the point of inflection of the velocity profile is located (see Fig. 9).

The expressions for the two main dimensionless critical characteristics—the wave number and the Reynolds number with respect to the external friction—contain the characteristic width of the shear L, which can be defined differently. For this reason, for the quantities characterizing the profile it is convenient to choose U_0, the characteristic (maximum) value of the velocity, and $U'(y_c)$, the derivative of the profile at the point of inflection $y = y_c$; these characteristics are determined uniquely from experiments. The the length scale L is expressed by the formula $L = U_0/U'(y_c)$, and the expressions for the Reynolds numbers with respect

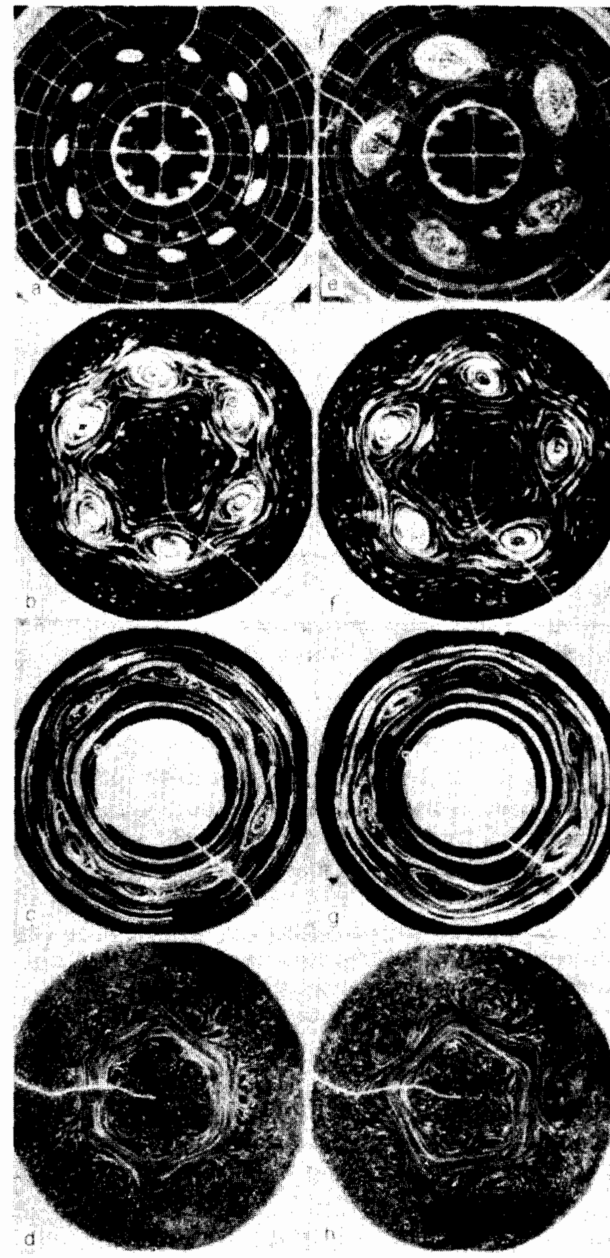

FIG. 10. Characteristic photographs of transcritical vortex regimes of flows for velocity profiles of the type sin y in an annular channel (a, e) and with "impedance" side boundaries (b, f), of the type tanh y (c, g), and jet flow (d, h).

to the external friction and the dimensionless wave number assume the form

$$R_\lambda = \frac{U'(y_c)}{\lambda} = \frac{U'(y_c) H_0^2}{2\nu}, \qquad \alpha = \frac{nL}{R_0} \tag{3.2}$$

TABLE III. The characteristics of flow with a narrow shear zone ($U = \tanh y$).

H_0, мм	L, см	n_0	α_0	R_ν^*	R_λ^*	H_0, мм	L, см	n_0	α_0	R_ν^*	R_λ^*
4	0.6,	7	0.40	32	8	4	0.7	6	0.40	50	8
5	0.65	7	0.44	32	8	5	0.8	5	0,38	48	9
3	0,55	7	0.37	42	7	3	0.8	5	0.38	122	8
4	0.65	7	0.44	35	8	4	0.85	4	0,35	62	8
5	0,75	5	0,37	38	8	5	0.9	4	0,33	52	8
3	0,6	7	0.40	65	8						

TABLE IV. The characteristics of flow in an annular channel ($U = \sin y$).

H_0, mm	L, cm	n_0	α_0	R^*_ν	R^*_λ
10	1.45	3	0.42	34	7
10	1.37	4	0.53	31	7
10	1.08	5	0.51	29	9
10	0.75	7	0,50	22	16
10	0.43	12	0,50	15	26

(R_0 is the radius of the point of inflection of the velocity profile or the maximum velocity of the jet).

We shall now describe the results. Table III gives the critical velocities of the parameters for a flow with a narrow shear zone.[77] The width L of the shear for the same constant depth H_0 was changed by changing the position of the cell above the magnet. One can see from the table that in a wide range of values of H_0 and λ the quantities R^*_λ and α_0 remain approximately constant, while R^*_ν varies from 32 to 125. The same constancy of R^*_λ and α_0 was observed in experiments with a sinusoidal flow with free boundaries[76] $R^*_\lambda = 7 \pm 1$ and $\alpha_0 = 0.5$ (in these experiments the width of the shear layer was varied with the depth held constant; R^*_ν ranged from 10 to 40), and for the jet flow[78] $R^*_\lambda = 7 \pm 1$, $\alpha_0 = 0.7$, and R^*_ν ranged from 10 to 45.

We note a result obtained in Refs. 73 and 77. In the case when the width of the channel is much greater than H_0 R^*_λ remains constant and equal to approximately 7. Decreasing the width of the channel, when it becomes comparable to the depth of the liquid, results in an increase of R^*_λ (Table IV). This is connected with the increase in the role of friction against the side walls of the channel.

Aside from investigations of the critical parameters, in Refs. 77 and 83 the characteristics of transcritical regimes were studied. One of the most important such characteristics is the amplitude A of the disturbance and its dependence on supercriticality. Since, as follows from experiment, the transition occurs in the soft regime of excitation, it should be expected that the square of this amplitude is proportional to the supercritically $s = (\mathrm{Re}/\mathrm{Re}^* - 1)$ (in this case it is not important how the Reynolds number is determined).

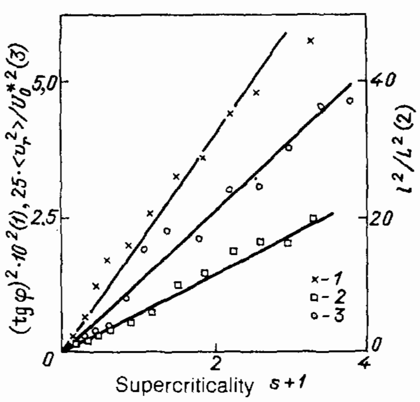

FIG. 11. The squared tangent of the slope angle of the vortex (1), the squared dimensionless width of the vortex (2), and the mean-square transverse velocity (3) as functions of the supercriticality for a flow of the type tanh y.

TABLE V. The coefficients of proportionality.

	$U = \tanh y$(1)	$U = \tanh y$(2)	$U = \sin y$
$\eta = \dfrac{\langle v_r^2 \rangle}{U_0^{*2} s}$	0,06	0,25	0,15
$\Phi = \dfrac{\mathrm{tg}^2\,\varphi}{s}$	0,02	0,025	0,06
$\Lambda = \dfrac{l^2}{L^2 s}$	5	6	14
$\dfrac{\Phi}{\eta}$	$\frac{1}{3}$	$\frac{1}{2}$	$\frac{2}{5}$
$\dfrac{\Lambda}{\eta}$	~85	~120	~95

The mean-square value of the radial velocity $\langle v_r^2 \rangle_\varphi$ on the neutral line (along the axis of the stream) as well as the width and slope angle of the vortex were measured from photographs of vortex flows with different values of Reynolds number. The streamlines near the center of the vortex are closed, nearly elliptical curves (see Fig. 10). The slope angle was determined as the slope angle of the major axis of the "ellipse" relative to the neutral line near the center of the vortex. It should be noted that near the center of the vortex different "ellipses" actually have the same slope angle φ. The width of the vortex l was taken to be the largest radial distance between the streamlines which bend around the vortex and pass through the hyperbolic points separating neighboring vortices. We shall show that these quantities characterize the amplitude of the disturbance.

Assume that to a first approximation the stream function of the disturbance is described by the formula

$$\psi = \int U\,dy + (Ae^{i\alpha x}\psi_1(y) + \text{c.c.}). \qquad (3.3)$$

Then for sufficiently small amplitudes the following estimates can be obtained for the tangent of the slope angle tan φ and for $\langle v_r^2 \rangle$:

$$\mathrm{tg}\,\varphi \approx 2\alpha A\,|\psi_1'(0)|, \qquad \langle v_r^2 \rangle \approx \alpha^2 |A|^2 |\psi_1(0)|^2. \qquad (3.4)$$

Experiments showed that the quantities $\mathrm{tg}^2\varphi$, l^2 and $\langle v_r^2 \rangle$ increase in proportion to supercriticality. Figure 11 demonstrates this dependence for a flow with a narrow shear zone (l is normalized to L while $\langle v_r^2 \rangle$ is normalized to the square of the characteristic velocity of the flow with the critical Reynolds number, U_0^*). The coefficients of proportionality calculated from the experimental data for the dependences presented are given in Table V.

The weak dependence (the relative constancy within the limits of experimental error) of the ratios Φ/η and Λ/η on the form of the velocity profile of the flow is interesting. It shows that the slope angle and the width of the vortices can indeed be used as a measure of the amplitude of the disturbance.

Figure 12 shows curves of $\langle v_r^2 \rangle$ and the amplitude of the average azimuthal velocity for a jet flow, also normalized to U_0^*. The experimental value of η was equal to 0.08. We call attention to the break in the dependence of the average azimuthal velocity on Re. It reflects the redistribution of ener-

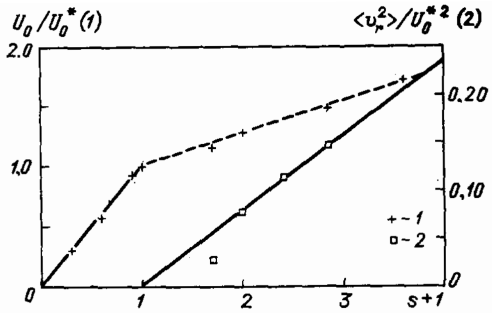

FIG. 12. The average longitudinal velocity (*1*) and squared transverse velocity (*2*) at the center of a jet as a function of the supercriticality.

gy from the main flow to the disturbance and was observed in flows with other types of velocity profiles.[73,74]

The flow with a jet-like velocity profile is distinguished by the existence of an easily measured characteristic—the azimuthal drift velocity of the vortices (Fig. 13). One can see that it also depends linearly on the supercriticality. Writing the drift velocity in the form $v_d = c_r + \omega_0 s/\alpha$—a sum of the "linear" drift velocity and a "nonlinear" correction (see Sec. 4.4)—it is possible to determine the quantities $c_r = 0.38 \pm 0.5$ and $\omega_0/\alpha = 0.18 \pm 0.03$.

Increasing further the Reynolds number results in instability of the flow with n_0 vortices and a reduction of the number of vortices. Transitions between flows with different symmetry indices are studied in detail in Subsec. 4.5. In addition, for large supercriticalities (as a rule, for $s = 10$–20) oscillatory flow regimes, connected with the simultaneous existence of two modes with different values of n, have been observed.

3.3 Comparison with the linear theory

As follows form the experimental results presented above, in particular, from the fact that for all flows described $R^*_\nu R^*_\lambda$, the linear theory of quasi-two-dimensional shear flows with external friction is applicable to the data obtained in the experiments. Indeed, in experiments with different flow parameters the critical values R^*_λ and α_0 remain the same, while R^*_ν varies over a wide range. The measured values $R_\lambda \approx 7$ are close to the value obtained in the linear theory $R_\lambda \approx 5$ and are virtually independent of the form of the profile. A disturbance with a finite wave number is most unstable, and in addition the experimental values $\alpha_0 \approx 0.4$ ($U = \tanh y$) and $\alpha_0 \approx 0.5$ ($U = \sin y$) are in good agreement with the theoretical values.

Good agreement with both the results of the given experiments and with the linear theory was found in Ref. 77 in the analysis of the experimental results obtained by other authors. For the Kolmogorov flow $R^*_\lambda = 8$ and $\alpha_0 = 0.64$. With regard to the experiments of Refs. 68–70 it first needs to be said that they refer to the degenerate case $R_\lambda = R_\nu$. Indeed, since the forcing action in them (velocity shear at the ends of the boundaries) has the character of a tangential discontinuity and is dissipated in the volume of the liquid by viscous forces, the characteristic width of the velocity profile is equal to the minimum width $L = L_{\min} = (\nu/\lambda)^{1/2}$ and the values of R_λ and R_ν are always equal. Nevertheless it turns out that the theory works even here, at the boundary of the region of applicability.

In the experiments of Ref. 69 the value $R^*_\lambda \approx 12$ was obtained for a stream flow and $R^*_\lambda \approx 15$ was obtained for a shear flow. The wave number α_0 turned out to be less than the theoretical values. The calculations performed in this work based on the linear theory showed that the increase in R^*_λ and the decrease in α_0 are related to the influence of internal viscosity.

In Ref. 70 the critical value of the Reynolds number was equal to $R^*_\lambda \approx 10$ and $\alpha_0 \approx 0.4$. Thus the influence of internal viscosity appears here also, but it is not as strong.

In Ref. 68 there is an additional factor that stabilizes the flow—the finite thickness of the disk that puts the fluid into motion. Indeed, by virtue of the Taylor-Proudman theorem, a vertical column of liquid strives to move without changing its height, i.e., in particular, without intersecting the cylindrical surface constructed above the edge of the disk. This could be why the values $R^*_\lambda \approx 30$–40 are much higher. However they do not change much when the external parameters are changed, and the value of α_0 remains equal to 0.4–0.5, as before.

Thus the experimental results presented show that the transition to instability is determined by the Reynolds number with respect to the external friction, and in addition R^*_λ and α_0 are virtually independent of the form of the velocity profile of the main flow. We also point out that in experiments with mixing layers[66] close values were obtained $\alpha_0 \approx 0.38$, and the dimensionless growth increments of the disturbances $\gamma \approx 0.2$ are close to the values obtained in the theory and in the experiments ($\gamma = 1/R^*_\lambda \approx 0.1$–$0.2$).

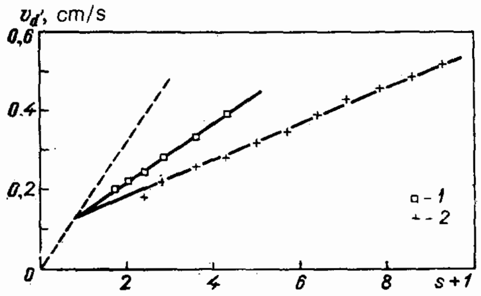

FIG. 13. The drift velocity of disturbances as a function of the supercriticality for the first mode $n = n_0 = 5$ (1) and for the second mode $n = 4$ (2).

4. NONLINEAR THEORY OF TRANSCRITICAL VORTEX REGIMES

4.1. The methods of the nonlinear theory applied to viscous flows

1. A powerful and universal practical method for solving the problems of mathematical physics is Galerkin's method. In this method the solution is represented approximately as a linear combination of a finite number of functions from some basis with undetermined coefficients and a system of ordinary differential equations for these coefficients is obtained. We recall that the famous system of Lorenz[84] was derived precisely as a Galerkin approximation of

the equations of hydrodynamics in the problem of rolling convection.

The classical formulation of the method for linear problems presupposes the use of the eigenfunctions of the stationary boundary-value problem as the natural basis, and this immediately leads to the optimal values of the coefficients in the expansion and automatically ensures that the boundary conditions are satisfied. The choice of the natural basis in nonlinear problems requires a special analysis. The main heuristic requirement on the choice of the basis is that Galerkin's method must give a dynamical system of minimum order with a given accuracy. It should be noted that even very simplified Galerkin dynamical systems can reflect correctly the qualitative behavior of the system being modeled (see Ref. 59). For example, the stability and transcritical regimes of a shear flow with a sinusoidal profile are described on the basis of a third-order dynamical system. This will be discussed in greater detail below.

One of the commonly employed methods for choosing a basis consists of using the set of eigenfunctions of the linear problem of stability (thus, for the problem of stability of a shear layer these will be the eigenfunctions of Rayleigh's equation). We note that if the rest state is taken as the main state (as in the case of convection), then the natural basis for hydrodynamic problems will be the set of eigenfunctions of Laplace's operator. This basis is often employed, but for the problem of the stability of shear flows it still requires taking into account a large number of terms in the expansion and integrating numerically the dynamical system obtained.[58,72] The problem is that neither the main flow nor the profile of the most general disturbance, as a rule, belong to the basis functions used for the expansion. There is, however, a special case, when both these functions are very close to the basis functions—this is the so-called Kolmogorov flow[53] $U = \sin y$. The application of Galerkin's method to it in Refs. 59, 85, and 86 made it possible, as was pointed out, to reduce the problem to a dynamical system of third order (triplet) and to trace the influence of external friction (see below).

2. For shear flows the Stewart-Watson method,[87,88] the idea of which goes back to the works of Poincaré and Landau, is often applied. It does not permit, like Galerkin's method, studying strongly transcritical regimes with self-excited oscillations and mode degeneracy, though it is not critically sensitive to the velocity profile of the main flow. The idea of the method consists of the following. The linear problem of stability is studied as the first term in the expansion in powers of the small amplitude A of the disturbance, the expansion is continued, and Landau's equation[10] is derived for the amplitude

$$\dot{A} = \gamma A + K_L |A|^2 A, \quad A \sim \varepsilon \ll 1. \tag{4.1}$$

The linear part of this equation describes the growth of the disturbance owing to the direct interaction with the main flow, and the nonlinear term describes the self-action of the disturbance, which can limit or enhance the growth in its amplitude depending on the sign of the Landau constant K_L. Physically the self-action is realized owing to the fact that because of the nonlinearity of the hydrodynamic equations a harmonic disturbance engenders its second harmonic, distorts the average profile of the longitudinal velocity of the flow, and then interacts with these secondary disturbances.

Technically the problem reduces to deriving and solving the equations for the disturbances up to second-order infinitesimals inclusively (for large Reynolds numbers $R_\nu \gg 1$ they have the form of Rayleigh's equations, but with a nonzero right side). After this the evolutionary equation for the amplitude is obtained as the condition that the third-order equation be solvable. Its coefficients, including Landau's constant, are expressed in the form of definite integrals of the first- and second-order disturbances.

In this review we omit a large number of investigations devoted to the Stewart-Watson method, its proof, and it applications to strictly two-dimensional flows. We shall confine ourselves here to only the most general considerations, which are important for what follows.

We note that if the terms in Landau's equation (4.1) are infinitesimals of the same order ($\sim \varepsilon^3$), then the time derivative and the linear increment γ must be of order ε^2. This means that such a weakly nonlinear theory can describe only slowly growing modes with wave numbers close to the neutral wave numbers (for $R_\lambda = 0$ they are $\alpha = 0$; α_s are the left- and right-hand boundaries of the region of unstable wave numbers; see Fig. 4). But real flows evolve primarily owing to the most unstable modes (which, generally speaking, are not "slowly growing"), so that results that are comparable to experiment cannot be obtained in this manner (this can be seen in the corresponding papers; see, for example Refs. 8 and 9).

There are several ways to make the increment of the most unstable disturbance small. High viscosity ($R_\nu \sim 1$) suppresses the short-wavelength disturbances (Fig. 5a), but it makes the problem more complicated, increasing the order of the equations, since the linear problem of stability reduces to the Orr-Sommerfeld equation. Stratification and the β-effect, conversely, leave disturbances with wave numbers close to the second neutral wave number $\alpha \gtrsim \alpha_s$ unstable. The corresponding amplitude equations are constructed in Refs. 89 and 90. Another method for limiting the region of unstable wave numbers and reducing the increments is to confine the flow in a narrow channel, which also suppresses growth of long-wavelength disturbances (without affecting the short-wavelength disturbances).[58,91] Finally, a flow in an annular channel, under conditions when only one wave number out of a discrete series of admissable values falls into the unstable region, and moreover near the critical wave number α_s, was studied in Ref. 92.

External friction also permits making the increment of the most unstable mode small, if the Reynolds number R_λ is close to the critical value. In this case, however, the form of the dispersion curve does not change, and the mode with $\alpha = \alpha_0$ remains the most unstable mode (see Fig. 5b). This fact turns out to be very important for the theory.

The main technical problem of the Stewart-Watson method, the problem of regularizing the critical layer, is related with the closeness of the wave number of the disturbance under study to the critical value (with $\lambda = 0$). From the mathematical viewpoint the critical layer is a singular point y_c of Rayleigh's equation (2.3) at which the denominator vanishes. If the wave number is close to the critical wave number, $c_i = 0$ (we recall that $c = c_r + ic_i$ is the complex phase velocity of the disturbance), then the critical point is close to the real axis, and although the numerator $U''(y_c)$ also vanishes for the traditionally studied antisymmetric velocity profiles $U(y) = -U(-y)$, the singularity still appears in the next orders of the expansion. To join the solution of Rayleigh's equation to the right and left of the singularity, special expansions of different type are constructed in the critical layer, depending on which of the terms in the equation is dominant—the viscous, nonlinear, or non-steady-state term.

We recall that in the presence of external friction and for $R_\nu \gg 1$ the right side of (2.8) can be neglected, and in this case the equation of liner stability reduces to Rayleigh's equation

$$\left[U-\left(c_{r\lambda}+ic_{i\lambda}+\frac{i}{\alpha R_\lambda}\right)\right](\varphi''-\alpha^2\varphi)-U''\varphi=0, \quad (4.2)$$

The significant difference introduced by external friction lies in the fact that the term $i/\alpha R_\lambda$, appearing in Eq. (2.8) or (4.2) shifts the singular point into the complex plane, and this term is not small if R_λ is close to the critical value R_λ^*. As a result the problem of the critical layer does not arise. At the same time, it is necessary to solve Rayleigh's equation with a nonzero right side and complex coefficients. This can probably be done analytically only for a piecewise-linear velocity profile $V(y)$, while for profiles of other types numerical methods must be employed. Such calculations for flows with $U = \tanh y$ and $U = \coth^{-2} y$ (taking into account the β-effect) were performed in Ref. 60. A comparison with the experiment of Ref. 69 showed good agreement. However only the linear characteristics of stability—the critical Reynolds number and the wave number of the most unstable mode—were compared. In Ref. 61 Landau's constant was calculated for a piecewise-linear profile and a collection of smooth profiles in order to compare with the experiment of Ref. 77, in which the growth of the amplitude of the disturbance as a function of the Reynolds number was measured for the first time for quasi-two-dimensional flows. This made it possible to observe the new effects described in Subsections 4.3 and 4.4.

4.2. Description of the transcritical regimes of a Kolmogorov flow

The problem of studying the stability of a two-dimensional flow driven by a spatially periodic force (the velocity profile $U = \sin y$, $-\infty < y < \infty$) was posed by A. N. Kolmogorov at a seminar he directed.[53] Because of the spatial periodicity it was possible to develop the theory of the Kolmogorov flow significantly farther than for shear flows of a general form. The dimensionless equation for the stream function in the case when there is no external friction has the form

$$\Delta\dot{\Psi}+[\Delta\Psi;\Psi]=\frac{1}{R_\nu}(\Delta^2\Psi+\cos y). \quad (4.3)$$

Representing the solution in the form of a sum of the main flow and a small perturbation, which is harmonic as a function of the longitudinal coordinate x with period $2\pi/\alpha$, we obtain the Orr-Sommerfeld equation for the transverse structure of the disturbance. Then, representing the disturbance in the form of a Fourier series in y, the linear problem of stability can be reduced to an infinite system of algebraic equations for the coefficients of this series; this problem can be studied by the methods of the theory of continued fractions. A linear theory of the Kolmogorov flow was constructed in Refs. 53 and 93. From this theory it follows, in particular, that the most unstable modes are the disturbances with small wave numbers $\alpha \to 0$, and for $\alpha > 1$ there are no instabilities. According to Refs. 53 and 93 the critical Reynolds number is $R^*_\nu = 2^{1/2}$, and the components of the Fourier series for the disturbance decay rapidly as $\alpha \to 0$. The latter fact makes it possible to represent the solution, to a first approximation, in the form

$$\Psi=\Psi_0(t)\cos y+\sum_{-1}^{1}\psi_n(t)\exp[i(ny+\alpha x)]. \quad (4.4)$$

Denoting

$$\Psi_0(t)=U(t),\quad z_0=i\alpha\psi_0,\quad z_+=i\alpha(\psi_1-\psi_{-1}),$$
$$z_-=\frac{i\alpha}{2}(\psi_1+\psi_{-1}), \quad (4.5)$$

we obtain the following dynamical system:[59,85]

$$\begin{aligned}
&\dot{U}+\frac{4}{\alpha}z_0z_1=R_\nu^{-1}(1-U),\\
&\dot{z}_0-\alpha U z_-=\frac{\alpha^2 z_0}{R_\nu},\\
&\dot{z}_--\alpha\left(\frac{1}{2}-\alpha^2\right)z_0U=-\frac{(1+\alpha^2)z_-}{R_\nu},\\
&\dot{z}_+=-\frac{z_+}{R_\nu}.
\end{aligned} \quad (4.6)$$

After the decaying component z_+ is eliminated there remains a very simple system of the hydrodynamic type (SHT)-a triplet,[59] which for

$$R_\nu<R_\nu^*=\sqrt{2}\left(1+\frac{2}{3}\alpha^2\right)$$

has a stable stationary solution $U = 1$, $z_0 = z_- = 0$, corresponding to the main flow. For $R_\nu > R_\nu^*$ it becomes unstable and a secondary flow with the following stream function is established:

$$\Psi=-\frac{R_\nu^*}{R_\nu}\cos y-\frac{[R_\nu^*(R_\nu-R_\nu^*)]^{1/2}}{\alpha R_\nu}\times\left(\sin\alpha x+\frac{2\alpha}{R_\nu^*}\sin y\cos\alpha x\right). \quad (4.7)$$

Using the method of the theory of branching, developed in Ref. 94 for the problem of the stability of spatially periodic flows, it can be shown that the expression (4.7) is the first term of the asymptotic expansion of the exact solution in a series in the small parameter $(R_\nu - R_\nu^*)^{1/2}$ around R_ν^*.

The properties of the steady-state solution (4.7) are studied in Ref. 97, where it is shown that it describes the qualitative structure of the flow observed in the experiment of Ref. 57, if the value of the dimensionless wave number $\alpha = 0.5$ close to the experimental value is used (we note that the linear theory does not give adequate grounds for making this choice, since the greatest supercriticality occurs in the absence of external friction at small wave numbers $\alpha \to 0$). However there are a number of discrepancies between this theory and experiment. Thus, according to the theory, as we have already mentioned, the most unstable modes should be the very long-wavelength disturbances. The critical Reynolds number, according to the experimental data, is $R_\nu^* \approx 2000$ and not $2^{1/2} \approx 1.4$. Finally, it is shown in Refs. 85 and

96 that the secondary steady-state and self-excited oscillatory regimes of the Kolmogorov flow with small α are unstable with respect to the smaller scale disturbances. In this respect the results of the direct numerical modeling performed in Ref. 97 are interesting. They show that long-wavelength modes can indeed be excited first in the flow, after which they are replaced by longer-wavelength modes.

These discrepancies can be eliminated by taking into account the external friction. The application in Refs. 57 and 59 of the methods of the linear theory, which were developed in Refs. 53 and 93, to Eq. (4.3) with the additional term $-\Delta\Phi R_\lambda$ on the right side (where for a thin layer λ is $2\nu/H_0^2$) showed that the curve of neutral stability has the form shown in Fig. 6 with the minimum corresponding to the most unstable wave number $\alpha_0 \approx 0.64$. The critical Reynolds number, according to the corrected theory, became $R_\nu^* \approx 1400$, which also approaches the experimental value. In this case Eqs. (4.6), supplemented with linear terms, which take into account the external friction (see Ref. 59), correctly describe the transcritical flow regimes.

It should be noted, however, that now the Galerkin approximation and the stream function of the secondary flow can no longer be regarded as the first terms of an exact asymptotic expansion, since the condition $\alpha \ll 1$ is not satisfied. For this reason the good agreement between the observed flow and the streamlines calculated according to Eq. (47) (Fig. 14—according to Refs. 95 and 59) is a lucky accident, due to which the next terms in the expansion turn out to be small.

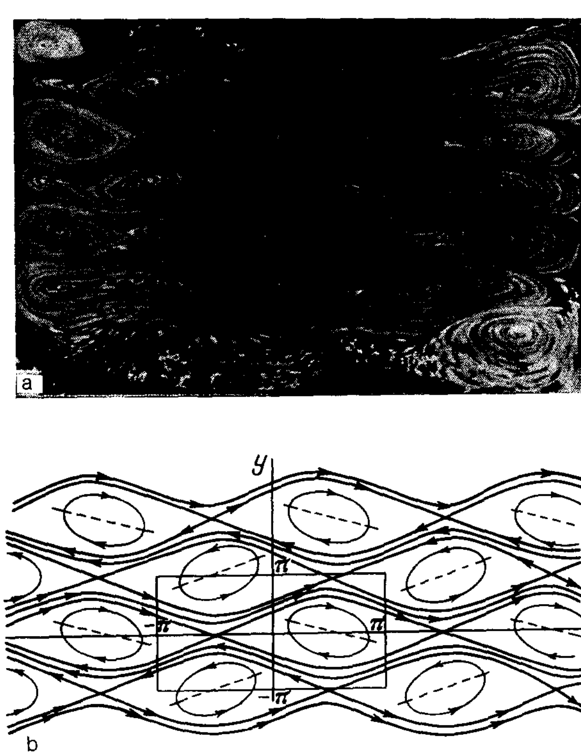

FIG. 14. Photograph of the transcritical regime (a) (Ref. 57) and the stream-lines calculated by Galerkin's method (b) (Ref. 95) for a Kolmogorov flow.

4.3. Model example with a piecewise-linear velocity profile

It was already pointed out above that the Stewart-Watson method is more effective for studying the stability of general shear flows. In this connection it is appropriate to study a well-known example that illustrates this method analytically and leads to, at first glance, a paradoxical result.

Piecewise-linear, or broken, velocity profiles $U(y)$ are distinguished by the fact that solving Rayleigh's equation for them reduces to solving the elementary equation $\psi'' - \alpha^2\psi = 0$ on the linear sections, where $U = 0$ (which gives $\psi = C_1 e^{\alpha y} + C_2 e^{-\alpha y}$), and determining the arbitrary constants $C_{1,2}$ from the conditions of joining at the break points of $U(y)$. The method of solving Rayleigh's equation for smooth profiles with the help of their approximation by a sequence of broken lines is, in particular, based on this.[98,99] Rayleigh himself obtained the solution of the linear problem of stability for an antisymmetric profile.

$$U = \begin{cases} -1, & y < -1, \\ y, & |y| < 1, \\ 1, & y > 1 \end{cases} \tag{4.8}$$

(see Fig. 4 and the formula (2.5)). The effect of weak viscosity ($R_\nu \gg 1$) on the linear stability of a flow with the velocity profile (4.8) was investigated in Ref. 100. It follows from the results presented in Ref. 100 that, in particular (weak) viscosity does not decrease, but rather increases the growth increment of the disturbances.

Since the Stewart-Watson method requires solving Rayleigh's equations it is very tempting to study analytically by this method a flow with the profile (4.8) in the presence of external friction. Such a study was performed in Ref. 61, but before we describe the results we must briefly discuss the mathematical difficulties arising here.

The solution of Rayleigh's equation (2.3) with the velocity profile (4.8) has the form

$$\varphi = \begin{cases} Ae^{\alpha y}, & y < -1, \\ Be^{\alpha y} + B^* e^{-\alpha y}, & |y| < 1, \\ A^* e^{-\alpha y}, & y > 1, \end{cases} \tag{4.9}$$
$$A = i - (1 + c_i^2)^{1/2} - c_i, \qquad B = ic_i A$$

(the asterisk denotes complex conjugation), where the wave number α and the phase velocity of the disturbance $c = ic_i$ are related by the dispersion relation (2.5) (in which $\gamma = \alpha c_i$). At the points $y = \pm 1$ the function (4.9) is continuous, but its derivative is discontinuous. At these points the second derivative $U''(y)$ has the form of a δ-function $U''(y) = \delta(y+1) - \delta(y-1)$, and this singularity must be compensated by the singularity of the second derivative $\varphi''(y)$. The function φ'', which appears explicitly in the further calculations, must thereby be written as the sum of a regular part and a singular part. Moreover, speaking imprecisely, we can say that the *same* δ-function that describes U'' appears in the expression for φ''. More precisely, this means the following.

Let $\theta_n(y)$ be a sequence of functions that converges to the Heaviside function $\theta(y) = y/|y|$ and $\delta_n = \theta_n'$. Then all integrals of the form

$$\int_{-\infty}^{\infty} \delta_n \theta_n^k \, dy \tag{4.10}$$

are determined and are equal to $1/k$. For this reason it can be assumed that the corresponding integral $\int \delta\theta^k dy$ is also determined for θ and the delta-function δ to which the sequence δ_n converges. This will not be the case, if δ and θ are defined by unrelated sequences of functions. Then expressions of the type $\int \theta\delta^k dy$ become "forbidden," as in the standard theory of generalized functions.

The fact that $U(y)$ and $\varphi(y)$ are related by Rayleigh's equation and for this reason have "the same" singularities is very important in the construction of a weakly nonlinear theory for the piecewise-linear velocity profile (4.8). The point is that the higher-order functions of the distubance have singularities already not only in the form of breaks, but also discontinuities and δ-functions. As a result the coefficients in Landau's equation are expressed in terms of integrals of the powers of a δ-function. By integrating by parts, however, taking into account Rayleigh's equation, they can be put into the form $\int \delta\theta^k dy$, and all final expressions are uniquely determined.

In this manner in Ref. 61 the following expression was derived for the critical Reynolds number R_λ^* in the presence of external friction and weak internal viscosity (R_ν^{-1} is of the order of the amplitude of the disturbance)

$$R_\lambda^* = \alpha c_i[1 - 2\alpha R_\nu^{-1}(1 - c_i^2)c_i^{-1}], \tag{4.11}$$

and Landau's equation was derived neglecting internal viscosity (we recall that c_i is given by the relation (2.5), in which $\gamma = \alpha c_i$)

$$\dot{A} = \alpha c_i s A + 3c_i(1 + c_i^2)^{1/2}\frac{1 + [c_i/(1 + c_i^2)^{1/2}]}{(4 + c_i^2)(1 + c_i^2)^2} A|A|^2 \quad (c_i > 0),$$

$$s = \frac{R_\lambda - R_\lambda^*}{R_\lambda^*}. \tag{4.12}$$

The expression (4.11) shows that a weak internal viscosity destabilizes the flow ($c_i < 1$). A similar effect of dissipation also appears in other physical situations, for example, in the case of Poiseuille flow, whose profile does not have inflection points, and the viscosity is the only source of instability. Here, for us, it is more important that Landau's constant in Eq. (4.12) is positive, so that the nonlinearity in this approximation does not stabilize the growth of the instability. This means that the excitation of the instability must be hard ("subcritical instability"), and the fifth-order term must be taken into account. However, in the experiments of Refs. 77 and 78, described in Sec. 3.2, the soft regime of excitation was observed, which clearly contradicts such a conclusion. The calculations performed in Ref. 60 for the profiles $U = \tanh y$ and $\coth^{-2} y$ gave the "correct" sign for the Landau constant. This makes it necessary to study the dependence of Landau's constant on the form of the velocity profile of the main flow, since, as we have seen, the effectiveness of the linear theory for a piecewise-linear profile does not guarantee that the results of the nonlinear theory will be in agreement with experiment.

4.4. The characteristics of the transcritical regimes of jet and shear flows

The characteristics of stability for a large number of smooth velocity profiles of the shear type were calculated in Ref. 61. The results are summarized in Table VI.

In this table the values of R_λ^*, α_0, and η, which is inversely proportional to Landau's constant (with the opposite sign) and measured in the experiments of Ref. 77 (see Sec. 3.2), are given. The numbers denote the corresponding velocity profiles:

1–4. Profiles with a linear section between the normalized "tails" of the hyperbolic tangent: two limiting cases 1) $U = \tanh y$ and 4) piecewise-linear; the cases 2 and 3 are intermediate between cases and 1 and 4.

5. $U = 3/4(\tanh y + 1/3\text{th}^{4/3} y)$—a profile for which $U'''(0) = 0$, i.e., close in a certain sense to a piecewise-linear profile.

6. $U = (2/\pi)\tan^{-1}(\pi y/2)$.

7. The profile of the flow of a viscous liquid driven by piecewise-linear force.

8. $U = \sin y$ with solid boundaries at $y = \pm\pi$.

From this table one can see that the linear characteristics of stability, as expected, depend relatively weakly on the form of the profile. At the same time, Landau's constant changes substantially, right up to a change in sign "in the neighborhood" of the piecewise-linear profile. It is especially instructive to compare the profiles 1 and 5, which, outwardly, are very close (the difference does not exceed 7%). The values of α_0 and R_λ^* for them are also close, and here Landau's constant differs by more than a factor of 5. What is the reason for this "sensitivity," i.e., the sensitivity of the nonlinear theory with respect to a change in the profile?

The formal reason[61] is that the third derivative φ''', which is directly related with U''' (through Rayleigh's equation), strongly affects the results. But for close functions $U(y)$ U''' can differ very strongly, which is what happens in this case. This can be given the following physical interpretation.[101]

We recall that by virtue of Helmholtz's theorem a particle of fluid in a nonviscous two-dimensional flow strives to preserve its vorticity. For a plane-parallel shear flow this means that the particle is "tied" to a definite value of the vorticity $\zeta = U'$. This restiction on the transverse displacements breaks down only on a streamline on which the gradient of the vorticity vanishes $\zeta' = U'' = 0$ (the existence of

TABLE VI.

№	1	2	3	4	5	6	7	8
α_0	0.46	0.45	0.43	0.40	0.45	0.65	0.38	0.57
R_λ^*	5.3	5.5	5.5	5.0	5.6	6.25	6.7	6.25
η	0.011	0.5	<0	<0	0.06	0.003	0.025	0.02

such a streamline therefore serves as a necessary condition for instability of flow—Rayleigh's criterion). But the amplitude of the transcritical regime, determined from the nonlinear theory, depends on the extent to which the particle can wander off its streamline. But this is now determined by the second derivative of the vorticity $\zeta'' = U'''$ at the point where the first derivative vanishes.

The effect of the strong dependence of Landau's constant on the form of the velocity profile of the main flow has several important consequences. First, it turns out that it is impossible to compare directly the theory with experiment, since it is practically impossible to determine reliably the actual profile of the flow velocity with an accuracy up to the third derivative. Second, in situations in which the velocity profile can change weakly, for one reason or another this can result in a significant change of the intensity of the vortices engendered by the instability. It is important that such a situation can be realized precisely in substantially quasi-two-dimensional flows, when the unifying effect of the internal viscosity on the velocity profile is minimum, and it completely repeats the profile of the acting force. We note in passing that the strong dependence of the intensity of the vortices on the shape of the profile could be one reason for the poor predictability of weather (see Sec. 5.4). Finally, the experimental data of Ref. 77, presented in Sec. 3.2, confirm the obtained result, since for two different velocity profiles with linear characteristics of stability, differing by not more than 20%, the values of η differ by a factor of 3 and are equal to 0.05 and 0.15, respectively.

The experimental values of η also agree in order of magnitude with the theoretical values. In particular, they are all small, $\nu \ll 1$, which explains the unexpectedly good applicability of the *weakly nonlinear* theory under conditions of very significant supercriticality $s = (\mathrm{Re}-\mathrm{Re}^*)/\mathrm{Re}$ (up to several units). Indeed, the characteristic magnitude of the dimensionless amplitude of the disturbance is $A \sim (\eta s)^{1/2}$, so that it remains small, and this is the condition of applicability of the theory.

Analogous results are also obtained for jet flows.[78] We shall consider here only the nonlinear characteristics. Aside from the amplitude of the disturbance (the theoretical values of η for the three velocity profiles studied fall in the range 0.025–0.05 and the experimental value is equal to 0.08), for jets there is one other parameter, easily measured experimentally and allowing comparison with theory. This is the drift velocity of the vortices. Its value of $R_\lambda = R_\lambda^*$ gives the real part of the phase velocity of the disturbance according to the linear theory, and the derivative with respect to Reynolds number is determined from the nonlinear theory. This derivative (in Ref. 78 it is denoted by ω_0/α) turned out to depend weakly on the form of the profile and is equal to 0.2, which is in good agreement with the experimental value of 0.19 ± 0.03.

Thus we can state that the nonlinear theory of stability, constructed taking the external friction into account, permits describing the main features of real shear flows.

4.5. Change of the vortex modes and the characteristic size of a vortex in developed quasi-two-dimensional flows

1. Up to now we have been discussing the development of only the most unstable mode with comparatively low values of the supercriticality. Meanwhile, the qualitative pattern of the behavior of strongly transcritical flows, when the number of vortices starts to change, is also a common feature of all experimental quasi-two-dimensional flows. This happens, as a rule, as follows. When the Reynolds number Re (here it is not important how Re is defined) increases quasistatically a stable principal mode with n_0 vortices is observed first. For some value $\mathrm{Re} = \mathrm{Re}_{n_0}^{(2)}$ this mode becomes unstable and there arises a flow with, in most cases, one less vortex: $n_1 = n_0 - 1$. When the Reynolds number reaches the next critical value $\mathrm{Re}_{il_1}^{(2)}$ this mode is in its turn replaced by the mode $n_2 = n_0 - 2$, and so on, until self-excited oscillations appear. When the Reynolds number "moves" back hysteresis is observed, i.e., the mode n_k is replaced by the preceding mode n_{k-1} with $\mathrm{Re} = \mathrm{Re}_{n_k}^{(1)} < \mathrm{Re}_{n_k}^{(2)} L$. From the diagram shown in Fig. 15 it is evident that hysteresis actually occurs, leading to nonuniqueness, i.e., the possibility of the existence of regimes having different numbers of vortices with one and the same Reynolds number—depending on the history of the flow and random factors (see below).

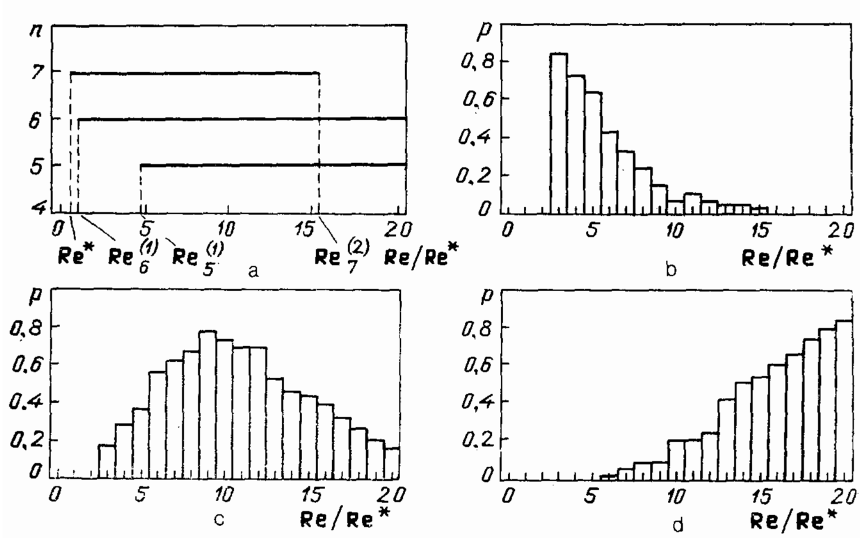

FIG. 15. Regions of existence of vortex regimes with different symmetry index (a) and the probabilities of obtaining these regimes by forcing ($b - n = n_0 = 7$, $c - n = 6$, and $d - n = 5$).[103]

It should be noted that other variants are also possible. Thus in Ref. 76 self-excited oscillations start immediately after the main flow becomes unstable, and in Ref. 74 the regions of stable stationary regimes alternate with transitional regions with self-excited oscillations (the number of vortices changes with the passage of time).[2)]

The mode changing processes were studied experimentally in Ref. 103, where it is shown, in particular, that the excitation of one of the possible regimes by impulsive forcing is of a stochastic character (see Fig. 15). The results obtained in studying the decay of a mode, when the Reynolds number moves quasistatically out of the region of existence of this mode, are of greatest interest. Under the experimental conditions the modes $n_1 = 6$ and $n_2 = 5$ were observed with $\mathrm{Re} = \mathrm{Re}_7^{(2)}$ and the modes $n_0 = 7$ and $n_1 = 6$ were observed with $\mathrm{Re} = \mathrm{Re}_5^{(1)}$ (see Fig. 15). It turned out that the probabilities of excitation of n_1 and n_2 with decay of the main mode n_0 (Re, increasing, passes through $\mathrm{Re}_7^{(2)}$) are equal to the probabilities of their excitation by impulsive forcing with $\mathrm{Re} = \mathrm{Re}_7^{(2)}$. The same thing happens with the decay of the mode $n_2 = 5$ on the left-hand boundary of the region of its existence.

These results can be interpreted[103] as evidence of the fact that the autonomous physical objects are not separate vortices, but rather vortex modes, which are created and decay as a whole. In the process, the transitions between regimes with different numbers of vortices occur not owing to the coalescence or fragmentation of vortices but rather as a result of the development of new, unstable modes from the random noise background, followed by their nonlinear competition and "survival of the strongest."[3)]

2. It is natural to try to describe transitions between modes (at least the first transition—with $\mathrm{Re}_{n_1}^{(1)}$) as resulting from the development of an instability of the secondary stationary flow. This can be done by two methods. First of all, the slow spatial change in the amplitude of the harmonic (along x) perturbation can be taken into account.[104] In this case the problem reduces to the Landau-Ginzburg equation

$$\dot{A} = \gamma A + DA_{xx} + K_{\mathrm{L}}|A|^2 A \qquad (A = A(x,\,t)), \qquad (4.13)$$

and the stability of the steady-state solution $A^2 = -\gamma/K_{\mathrm{L}}$ relative to periodic disturbances (the modulation instability) can be studied.

The second method is connected with a different generalization of the theoretical scheme of the Stewart-Watson method, when two disturbances with close wave numbers and independent amplitudes A_1 and A_2 are taken into account simultaneously. It leads to a system of two coupled Landau equations

$$\begin{aligned} \dot{A}_1 &= \gamma_1 A_1 + K_{11}|A_1|^2 A_1 + K_{21}|A_2|^2 A_1, \\ \dot{A}_2 &= \gamma_2 A_2 + K_{22}|A_2|^2 A_2 + K_{12}|A_1|^2 A_2. \end{aligned} \qquad (4.14)$$

Both methods are essentially equivalent, since the same disturbed flow can be represented as being the result of weak modulation or addition of a different mode:

$$e^{i\alpha x} + \varepsilon e^{i(\alpha+\Delta\alpha)x} = e^{i\alpha x}(1 + \varepsilon e^{i\Delta\alpha x}). \qquad (4.15)$$

Without going into details, we note only that this approach does not permit describing the most important feature of the phenomenon under study, namely, it turns out that the main mode $\alpha = \alpha_0$ does indeed become unstable at some $\mathrm{Re}^{(2)}$, but the quantity $\mathrm{Re}^{(2)}-\mathrm{Re}^*$ (where Re^* is the critical Reynolds number for the main flow) depends quadratically on $\Delta\alpha$—the wave number of the modulation (first method) or the difference of the wave numbers of the disturbance and the main mode (second method). The transitions to modes with smaller and larger wave number thereby turn out to be equivalent theoretically. But experiment, as we have already mentioned, almost always demonstrates a transition to a mode with a smaller wave number. It can be shown[105] that only a very special ratio of the coefficients in the system (4.14), which cannot be obtained on the basis of the approximation studied, could give this asymmetry. It is also unclear how the Landau-Ginzburg equation could be modified so that it would correctly describe the process of mode changing.

3. In Refs. 5, 69, 74, and 77 the reduction in the number of vortices with an increase of the Reynolds number is explained as follows. The back effect of the vortices on the average longitudinal flow results in broadening ("spreading") of the profile of the average velocity (this broadening was demonstrated experimentally in Ref. 78 for a jet). But for the widest profile the mode with the largest increment has the smallest wave number, which is what leads to the change of regime. This explains the physical mechanisms, but does not permit constructing a theoretical model. A different approach is more fruitful.

In Ref. 69 the increase in the characteristic size of a vortex is attributed to the so-called phenomenon of reverse cascade of energy in two-dimensional turbulence. In a two-dimensional liquid, as a result of the existence of an additional integral of the motion—the vorticity, the transfer of energy along the spectrum in the inertial interval proceeds from large wave numbers to small wave numbers, and not in the reverse direction, as in the three-dimensional case.[106]

In Ref. 107 it is noted that the effect of the Ekman friction on rotating two-dimensional turbulence reduces to establishing the left-hand boundary of the inertial interval, in other words, the maximum size of vortices in a two-dimensional turbulent flow. This size is[107] $D_\lambda = \bar{u}\tau_{\mathrm{E}}$, where $\bar{u}$ is the rms velocity of the turbulent pulsations, while $\tau_{\mathrm{E}} = H_0/(\Omega\nu)^{1/2}$ is the Ekman time. (It is obvious that we can write $D_\lambda = \bar{u}/\lambda$, having in mind a generalization to the case of nonrotating quasi-two-dimensional turbulence.) The size D_λ can be expressed in terms of the specific dissipation of turbulent energy ε, which gives[101]

$$D_\lambda = \left(\frac{\varepsilon^3}{\lambda}\right)^{1/2}.$$

Analogously to the Kolmogorov-Obukhov inner scale in three-dimensional turbulence[108] $d_\nu = (\nu/\varepsilon^3)^{1/4}$ the "outer" scale D_λ determines the size of the vortex for which the characteristic time of one revolution is of the order of the dissipation time—large (smaller) vortices in two-dimensional (three-dimensional) turbulence simply cannot exist. However, the left-hand end (with respect to the wave number) of the inertial interval, in contrast to the right-hand end, is the energy-containing interval and for this reason D_λ can be regarded not simply as the maximum size of vortices, but as the characteristic size of vortices.

We now note that the rate of dissipation of energy on the left-hand end of the inertial interval (ε) is equal to the rate of generation of energy by the external source, which, as in the case of three-dimensional turbulence (see, for example, Ref. 108), can be estimated in terms of Reynolds number. As a result the following estimate is obtained for D_λ:[109,110]

$$D_\lambda \sim R_\lambda^{3/4} L \qquad (4.16)$$

(L, as previously, is the characteristic width of the shear).

The derivation of this dependence reduces to evaluating the terms in the starting equation (1.7) and does not require any assumptions other than the existence of the inertial interval (in which energy generation and dissipation are insignificant). For this reason the formula (4.16) can be applied to nonturbulent shear flows for describing the growth of vortices with increasing Reynolds number. These experiments[68,69,77,79,80] confirm the dependence (4.16). In particular, Fig. 16 shows the dependence (converted to logarithmic coordinates) of the dimensionless wave number on the Reynolds number according to the data of Ref. 69. The straight line in this figure has a slope of $-3/4$, which corresponds to the dependence (4.16). It was drawn along the lower boundary of the "cloud" of experimental points, since the dependence (4.16) describes the *maximum* size of a vortex, i.e., the *minimum* wave number (see also Fig. 21 in Sec. 5.3). Thus external friction is the determining factor not only for weakly transcritical but also for developed quasi-two-dimensional flows.

In conclusion we shall give an estimate[101] of the scale D_λ for the earth's atmosphere. Taking $\varepsilon = 5\ \mathrm{cm^2/s^3}$ (see, for example, Ref. 111) we obtain $D_\lambda \approx 1500$ km, which is the characteristic size of large-scale atmospheric motions (see also the remark[6)] mentioned below).

5. GEOPHYSICAL APPLICATIONS

5.1. The effect of the Ekman layer on the stability of Rossby waves

As follows from the similarity criteria presented in Sec. 1.4, under certain assumptions the earth's atmosphere can be regarded as a thin layer of a nonviscous, incompressible, rotating fluid. The fact that this fluid is "poured" on the surface of a sphere plays a significant role in large-scale atmospheric motions. As a result the effective rotational frequency is equal not to $\Omega_0 = 2\pi/\mathrm{day}$ but rather to the projection on the normal to the earth's surface $\Omega_0 \sin\varphi$, where φ is the geographical latitude. As a result each particle of fluid, striving to conserve vorticity, turns out to be fixed on its own parallel, and when it is deflected along the meridian a return force arises. This is the mechanism of the oscillatory motion in Rossby waves.

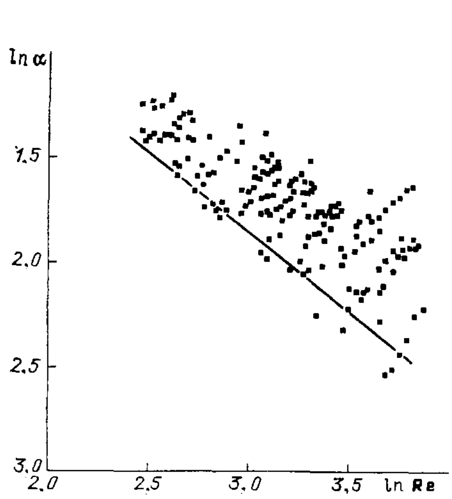

FIG. 16. The dimensionless wave number as a function of the Reynolds number in the experiment of Ref. 69 on a logarithmic scale. The slope of the straight line is equal to $-3/4$.

Since transverse motions are concentrated in a small interval of latitudes, to study the stability of Rossby waves it is sufficient to use the β-plane approximation, in which the stream function of an elementary Rossby wave (neglecting two-dimensional compressibility, $kL_0 > 1$) has the form

$$\psi = A\cos[k(x+ct)], \qquad c = \frac{\beta}{k^2}. \qquad (5.1)$$

This solution of the Obukhov-Charney equation describes a periodic shear flow, related to the Kolmogorov flow, but with an explicit time dependence. Such a shear flow may turn out to be barotropically unstable; this was first pointed out by Lorenz[44] in connection with the problem of the predictability of atmospheric motions. The decay and parametric mechanisms in the "nonviscous" theory of instability were studied in a series of subsequent works (see references in Ref. 39). Here we shall consider the question of the effect of the Ekman friction on the barotropic instability of Rossby waves.[39]

As in the case of the Kolmogorov flow, the equation of the linear problem of stability (linearization of Eq. (1.23) relative to (5.1)) has periodic coefficients, which makes it possible to seek the solution in the form of a Fourier series. The infinite system of algebraic equations for the coefficients of this series is solved by the continued-fraction method proposed in Ref. 53 and extended in Ref. 39 to the case of complex coefficients (their imaginary parts differ from zero owing to the β effect). The stability of the wave relative to disturbances periodic in x and y with period along the longitudinal coordinate x that is a multiple of the period of the wave itself, was studied. The threshold of stability with respect to the amplitude of the velocity is given by the formula

$$v_{\text{кр}}^2 = A_{\text{cr}}^2 k^2 = \frac{2\left[(l^2+k^2)^2\lambda^2 + c^2k^2l^4\right]}{l^2(k^4-l^4)},$$

where λ is the coefficient of Ekman friction and l is the transverse wave number of the superposed disturbance.

The result is presented in Fig. 17 in the form of neutral curves in the coordinates "transverse wave number-wave amplitude" taking into account and neglecting the external friction (for the parameters of the real atmosphere of the earth). One can see that the external friction, as in the previously studied cases, does not simply increase the threshold of stability (in this case—from zero to a finite value), but it also separates the most unstable wave number. It is significant that the Rossby wave with amplitude 12 m/s and global wave number (the number of periods fitting into the latitude circle) $n_0 = 6$, given by Lorenz[44] as typical, turns out to be unstable in the absence of external friction and stable when external friction is taken into account (circle in Fig. 17). It should be noted that Rossby waves, being a large-scale element of the general circulation of the atmosphere, carry information about the weather. For this reason, it is very important to take Ekman friction into account when describing the Rossby waves.

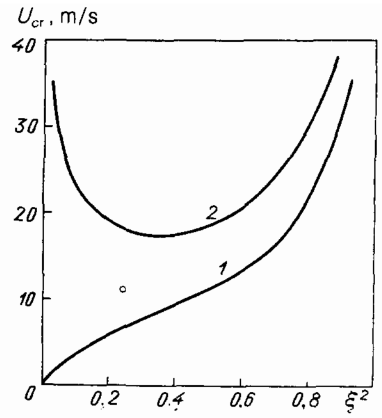

FIG. 17. The critical curves for Rossby waves with dimensionless wave number $n = 6$: *1*) according to nonviscous theory,[44] *2*) taking into account the Ekman flow.[39] ξ is the dimensionless transverse wave number of the disturbance.

5.2. The three-dimensional structure of the quasi-two-dimensional flows of a rotating fluid

Since for the atmosphere Ekman's number $E = \nu/\Omega H_0^2$ is small, the structure of the flows in it has a number of characteristic features, the most important of which is the appearance of boundary layers on solid surfaces and above singularities in the boundary conditions (this could be breakdown of smoothness of the bounding surfaces, sharp velocity shears or localized sources and sinks of mass). Different examples of boundary layers of this type can be found in the book of Ref. 36. Here we shall concentrate our attention on the question of the extent to which the motion of a rotating fluid can be regarded as two-dimensional. In this connection we shall study the "fine structure" of the steady-state zonal shear flow of a rotating liquid under the traditional assumption that the Rossby $\mathrm{Ro} = U_0/L\Omega$ and Ekman numbers are small.

In this case the smallness of Ro makes it possible to linearize the Navier-Stokes equations with respect to the fast general rotation. The small Ekman number, however, appears as a coefficient in the terms with the highest-order derivative (viscous terms), as a result of which the problem can be separated into two problems—for the boundary layer on horizontal boundaries (on the bottom and, possibly, on the cover—these are the Ekman layers) and for the "free atmosphere" outside the boundary layers. Then the circulation in the free atmosphere, taking the Ekman layer into account, is described by the following equations (see, for example, Ref. 36):

$$\begin{gathered} E\partial_y^2 u - 2\partial_z \chi = 0, \quad E\partial_y^4 \chi + 2\partial_z u = 0, \\ 2(\chi(y,0) - \chi_{\text{в}}(y)) = -E^{1/2}(u(y,0) - u_{\text{в}}(y)), \\ 2(\chi(y,1) - \chi_{\text{н}}(y)) = -E^{1/2}(u(y,1) - u_{\text{н}}(y)), \end{gathered} \tag{5.2}$$

where u is the longitudinal (zonal) velocity, χ is the stream function of the transverse circulation in the meridional plane (y,z) (do not confuse with the horizontal stream function!), $\chi_{t,b}$ and $u_{t,b}$ are the boundary values at the top and bottom boundaries, and the lengths are normalized to the depth of the fluid. These equations were obtained by the usual method of joined asymptotic expansions. They refer to a problem that is homogeneous along the longitudinal coordinate x. The cylindrically symmetric case can be studied analogously.

We note that it follows immediately from the form of the boundary conditions that a flow can be excited, with equal success, by the differential motion of boundaries (u) or by sources and sinks of mass at the boundaries (χ).

Analysis of Eqs. (5.2) shows[34,35] that there are two characteristic scales $\delta_S^{(3)} = E^{1/3}$ and $\delta_S^{(4)} = E^{1/4}$. If the characteristic distance over which the boundary conditions change greatly exceeds the largest of them $\delta_S^{(4)}$), then the terms with the small parameter E in Eq. (5.2) can be neglected, and the flow is two-dimensional, $\partial/\partial z = 0$. In laboratory experiments, however, it is much more convenient to work with discontinuous boundary conditions—when separate annular sections of the bottom move with different velocities, or sources and sinks of mass, localized on circles are present (discontinuity in the boundary values of u or χ, respectively). In this case free Proudman-Stewartson layers arise above the discontinuities. They have a double structure: in the inner sublayer $\delta_S^{(3)}$ the viscous forces smooth the discontinuity of the vertical velocity while in the outer sublayer $\delta_S^{(4)}$ they smooth the discontinuity of the zonal velocity. Thus intense vertical motions occur predominantly in the Proudman-Stewartson layers, and the entire transverse circulation is concentrated in the Ekman and Stewartson boundary layers (a diagram of the transverse circulation for the case of a jet flow excited between the annular source and sink of mass, as in Ref. 80, is presented in Fig. 18b). In the inner sublayer the dependence on the vertical coordinates is already significant. To establish how significant this dependence is, it is necessary to solve the system (5.2).

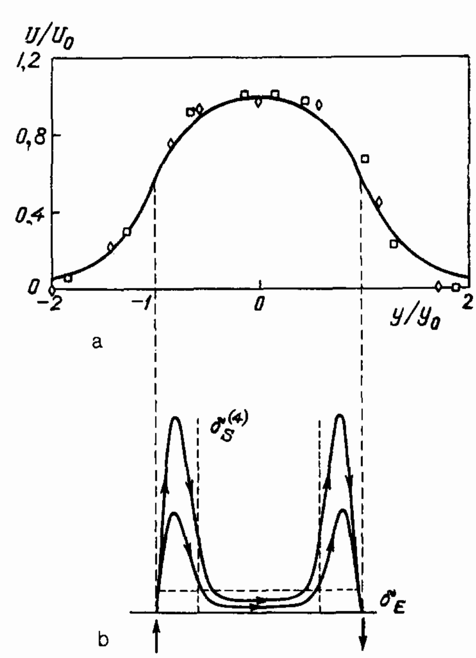

FIG. 18. a) Theoretical (curve) and experimental (dots) velocity profiles of the jet in Fig. b;[80] the velocity is normalized to the maximum value and the transverse coordinate is normalized to the position of the sources and sinks. b) Schematic diagram of the streamlines of transverse circulation for a jet exicted in a rotating fluid by a source and sink (arrows). The Ekman (δ_E) and Stewartson (δ_S) layers in which the transverse circulation is concentrated are indicated.

The solution of the system (5.2) is sought with the help of a Fourier transformation with respect to the transverse coordinate y. Then the Fourier integrals obtained can be employed to obtain the asymptotic expansions (as $E \to 0$) of the series[36,69,79] approximating $u(y,z)$ and $\chi(y,z)$. However these series converge very poorly in the region, of interest to us, near the discontinuity in the boundary condition. For this reason it is better to study the asymptotic behavior of the solutions in this region starting directly from their integral representation. By this method it can be shown[80] that even in the inner Proudman-Stewartson layer the dependence on the vertical coordinate is significant only in an asymptotically small region $z < E^{1/8}$, $|y - y_0| < E^{3/8}$ (y_0 is the position of the discontinuity). This makes it possible to regard, with good accuracy, the flow in the experimental apparatus as two-dimensional and to calculate its profile. The theoretical and experimental velocity profiles according to the data of Ref. 80 are compared in Fig. 18a.

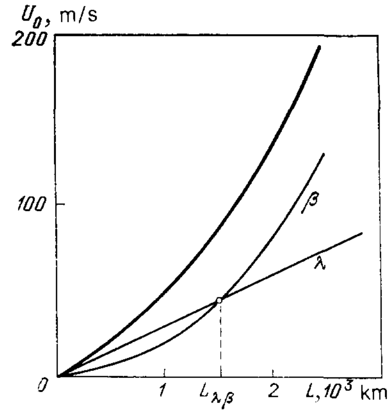

FIG. 19. The neutral curves for a shear flow under the influence of external friction (curve λ), the β effect (curve β), and both factors together (thick curve)[101] with the values of λ and β characteristic for the earth's atmosphere.

5.3. Effect of differential rotation

The β effect, which leads to the appearance of Rossby waves, also significantly affects the stability of latitudinal flows. Indeed, the total vorticity is now equal to $U' - f$, where f is the Coriolis parameter (the doubled effective rotational velocity of the system as a whole; the minus sign is connected with the chosen direction of the axes and the earth's actual direction of rotation, and for instability of shear flow it is now required that somewhere the sum $U'' - \beta$ should vanish, where $\beta = f'$ appears in Eq. (1.14). This generalization of Rayleigh's criterion was obtained by Kuo in Ref. 112.

It is obvious that the β effect can in principle suppress the instability of the shear flow, if $\beta > \max U''$.[4)] For this reason it is important to clarify the role of external friction compared with the β effect in the real atmosphere. This was done in Ref. 101; here we can confine ourselves to a qualitative analysis only.

Let the velocity profile $U(y)$ of the main latitudinal flow be fixed and let only its amplitude U_0 and width L vary: $u(y) = U_0 U(y/L)$. We shall assume that the profile is antisymmetric and normalized so that $U'(0) = |U(\pm\infty)| = 1$. We denote $m \equiv \max U''$. We shall determine the form of the neutral curve of stability in the coordinates (L, U_0). In the absence of external friction stability is determined by the modified Rayleigh criterion, in accordance with which the critical velocity is expressed by the formula

$$U_0^* = \frac{\beta L^2}{m} \tag{5.3}$$

(the corresponding parabola in Fig. 19 is marked with the letter β). On the other hand, in the absence of the β effect the critical velocity is

$$U_0^* = R_\lambda^* \lambda L = \frac{\lambda L}{\gamma_0}, \tag{5.4}$$

where γ_0 is the maximum linear increment for the profile $U(y)$, obtained from the solution of Rayleigh's equation (the curve λ in Fig. 19). It is obvious that the total neutral curve taking into account both stabilizing factors passes above these two curves and asymptotically approaches Eq. (5.3) for large L and Eq. (5.4) for small L. In other words, there exists the characteristic scale $L_{\lambda\beta} = m\lambda/\gamma_0\beta$ (the point of intersection of the curves (5.3) and (5.4), such that for $L > L_{\lambda\beta}$ the β effect predominates and for $L < L_{\lambda\beta}$ the external friction predominates. For estimates we shall use the values of λ and β, presented in Sec. 1, for the earth's atmosphere at middle latitudes, and the characteristic value $\gamma_0 \approx 0.2$, and we note that the minimum possible value of m for antisymmetric monotonic profiles is $m_{\min} = 1/2$ (it is achieved on the profile with a piecewise-constant second derivative; the maximum value $m = \infty$ corresponds to the piecewise-linear profile). This estimate gives

$$L_{\lambda\beta} = \frac{(1/2) \cdot 5 \cdot 10^{-6}\ \mathrm{s}^{-1}}{0.2 \cdot 1,6 \cdot 10^{-9}\ \mathrm{m}^{-1}\mathrm{s}^{-1}} \approx 1000\ \mathrm{km}, \tag{5.5}$$

and in addition, since here the minimum value of m was used, this is a lower limit. Hence, under the conditions of the earth's atmosphere external friction cannot be neglected, even for the flows with the largest scales.[5)]

The influence of the β effect on the stability of shear flows was studied experimentally in Ref. 80 on the example of a jet (we recall that the β effect arises in a fluid whose depth varies as a function of the radius). The parameters of the apparatus made is possible to generate flow with $L \gg \lambda_{\lambda\beta}$, and the results thus fall primarily on the curve (5.3) (Fig. 20; in this figure the dots show all the observed stable regimes and not only those that are close to the neutral curve). It should be noted that although the theoretical profile of the flow velocity agrees well with the experimental profile (see

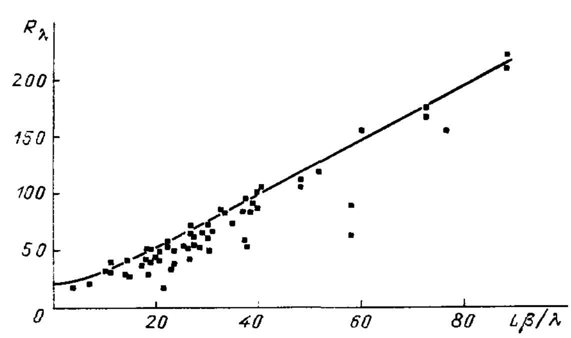

FIG. 20. Diagram of stability of a jet flow:[80] the dots denote the observed subcritical regimes.

Subsection 5.2), the value of the dimensionless maximum of the second derivative m, calculated from the experimental data on stability with the help of the formula (5.3), was equal to $m_{\exp} \approx 1/2$ and not $m = 2$, as if found from the theoretical profile. This shows once again how sensitive the characteristics depending on the higher order derivatives can be to "small" differences between the experimental and theoretical profiles.

The β effect also affects strongly transcritical, including turbulent, flows, since as the scale of the vortices increases they start to transform into Rossby waves. In the investigations devoted to this phenomenon (Refs. 28 and 29; see also the review of Ref. 113) it is shown that this occurs on scales of the order of $\varepsilon^{-1/5}\beta^{-3/5}$ (ε is the specific dissipation) and results in the formation from isotropic turbulence of structures, stretching in the latitudinal direction. From here it follows that in the presence of the β effect the formula for the characteristic size of vortices in developed quasi-two-dimensional flows (4.16) must be modified. Apparently two characteristic dimensions must appear—in the latitudinal and longitudinal directions. In addition, in bounded vessels an alternative mechanism of dissipation—transport of energy by Rossby waves to the side walls[6)]—must be taken into account.

The formula (4.16) nonetheless is applicable also for the experiments of Refs. 79 and 80, in which a jet in the β plane was modeled (the graph of the dependence of the wave number on the supercriticality, constructed in Refs. 109 and 110 using the results of Ref. 80, is presented in Fig. 21). This is explained by the fact that Rossby waves, which can propagate only "westward," were channeled in these experiments in an "eastward" jet and could not carry off the energy of the flow to the side walls. For this reason external friction remained the main mechanism of dissiption.

CONCLUSIONS

The main physical conclusion following from the foregoing analysis that the characteristics of stability of quasi-two-dimensional shear flows can be divided into two groups: virtually independent of the form of the profile (in particular, the critical Reynolds number, the wave number of the most unstable mode) and sensitive to the form of the profile (the second Landau constant, responsible for the intensity of vortices in transcritical flows). This means that even weakly transcritical regimes of quasi-two-dimensional shear flows are poorly predictable, since under natural conditions some physical factors always contribute to changing the profile of the main flow. In the atmosphere, for example, the profile of the zonal flows is changed primarily by baroclinic effects as well as the interaction (though weak) of the motions in the boundary layer and in the free atmosphere.

If the appearance of the vortex structures can be explained by the small supercriticality of large-scale flows, with respect to which the small-scale turbulence plays a dissipative role, then their spatial-temporal variability is connected with the weak change in the velocity profile of the main flow. Since in the process the intensity of the vortices varies much more strongly than their size and form, such formations can be classified as coherent structures. This explains one of the main mechanisms of self-organization in turbulent flows.

In quasi-two-dimensional motions the reverse cascade of energy along the spectrum, bounded above by the scale D_λ, in which the main part of the kinetic energy is concentrated, also contributes to self-organization. With respect to external friction, owing to the small-scale tubulence, such motions are weakly transcritical (precisely because dissipation on the scale D_λ is related with external friction). Thus external friction plays a fundamentasl role in the formation of many hydrodynamic processes, which cannot be understood correctly if it is neglected.

We thank M. V. Nezlin for carefully reading the manuscript and for a number of valuable remarks.

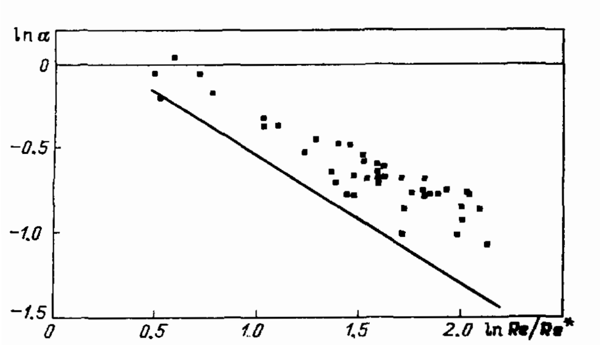

FIG. 21. The dimensionless wave number as a function of the Reynolds number for transcritical regimes of a jet flow[80] on a logarithmic scale. The slope of the straight line is equal to $-3/4$.

[1)]A barotropic fluid is a fluid whose equation of state is given by the dependence $p = p(\rho)$, i.e., the pressure is a function of the density only.

[2)]This unexpected result was obtained in the experiment of Ref. 102. According to Ref. 102, the lower boundaries of the regions of existence of the modes $\mathrm{Re}^{(1)}_{n_k}$ fall precisely on the neutral curve $\mathrm{Re}(\alpha)$. In the experiments of other authors, as Re decreases quasistatically the mode n_k becomes unstable before the critical Reynolds number, determined on the basis of the linear theory for the corresponding wave number, is reached. Nonetheless the result of Ref. 102 appears to be reliable, since the authors of this paper observed a reduction of the amplitude of the mode right up to the complete vanishing of the mode at the moment when $\mathrm{Re} = \mathrm{Re}^*_{n_k}$, as should happen when the neutral curve is reached. The preceding mode n_{k-1} was excited only after this. One possible explanation is that the carefulness in preparing the apparatus, to which great importance was attached in Ref. 102, reduces to a minimum the random perturbations necessary in order for the instability of the secondary transcritical flow to develop during the observation time (the characteristic time of this instability can be much longer than for the instability of the primary flow).

[3)]In some physical situations vortices can be regarded as autonomous objects. Thus under the conditions of the experiments of Ref. 5 screening at the Rossby-Obukhov radius effectively isolates vortices from one another. Strong turbulence possibly plays an analogous role in Refs. 81 and 82. We note that in both cases it is possible to observe regimes with one localized vortex.

[4)]We note that the form of the velocity profile plays a significant role here also. Thus the "angular" profile of the piecewise-linear type is not stabilized by the β effect.

[5)]It is interesting that from the results of Ref. 92, in which the main stabilizing factor was the β effect and external friction was taken into account as a small correction, it follows that even in this case the friction fundamentally changes the behavior of the steady-state transcritical regimes.

[6)]Here it should be noted that in the real earth's atmosphere quite a number of mechanisms capable of affecting in some way the characteristic size of vortices is present. It is remarkable that the corresponding scales of the dimension of length—the earth's radius, the Rossby-Obukhov radius, the "outer" scale of turbulence, and the scale $\varepsilon^{-1/5}\beta^{-3/5}$ mentioned above—are close in order of magnitude. This, in particular, determines the extreme complexity of the atmosphere as an object of research.

[1]D. Fultz, in *Compendium of Meteorology* (Ed. J. F. Malone), Am. Meteorol. Soc., Boston, 1951, p. 1235.
[2]R. Hide, Q. J. R. Meteorol. Soc. **79**, 161 (1953).
[3]R. Hide and P. T. Mason, Adv. Phys. **24**, 47 (1975).
[4]F. V. Dolzhanskiĭ and G. S. Golitsyn, Izv. Akad. Nauk Fiz. Atmos. Okeana **13**, 795 (1977) [Izv. Acad. Sci. USSR Atmos. Oceanic Phys. **13**, 550 (1977)].
[5]M. V. Nezlin, Usp. Fiz. Nauk **150**, 3 (1986) [Sov. Phys. Usp. **29**, 807 (1986)].
[6]M. V. Nezlin and E. Snezhkin in: *Nonlinear Waves: Structures and Bifurcations* [in Russian] (Eds.) A. V. Gaponov-Grekhov and M. I. Rabinovich, Nauka, M., 1987.
[7]P. G. Drazin and W. H. Reid, *Hydrodynamic Stability*, Cambridge Univ. Press (1981).
[8]P. Heurre, Philos. Trans. R. Soc. London, No. 1408, 643 (1980).
[9]F. H. Busse, J. Fluid Mech. **33**, 577 (1968).
[10]L. D. Landau and E. M. Lifshitz, *Fluid Mechanics*, Pergamon Press, N. Y., 1959 [Russ. original, GITTL, M., 1954 and Nauka, M., 1986].
[11]C.-G. Rossby *et al.*, Bull Am. Meteorol. Soc. **18**, 201 (1937).
[12]A. M. Obukhov, Izv. Akad. Nauk SSSR, Ser. geograf. geofiz. **13**, 281 (1949).
[13]J. Pedlosky, Geophysical Fluid Dynamics, Springer-Verlag, N. Y., *1979* and *1987* [Russ. transl., Mir, M., *1984*].
[14]H. Ertel, Meteorol. Z. **59**, 277 (1942).
[15]N. E. Kochin, I. A. Kibel', and N. V. Roze, Theoretical Hydromechanics, Interscience, N. Y., 1964 [Russ. original, Fizmatgiz, M., 1963.
[16]A. M. Obukhov, N. E. Kochin and the Development of Mechanics [in Russian], Nauka, M., 1984, p. 84.
[17]M. V. Kurganskiĭ and M. S. Tatarskaya, Izv. Akad. Nauk SSSR Fiz. Atmos. Okeana **23**, 787 (1987) [Izv. Acad. Sci. USSR Atmos. Oceanic Phys. **23**, 587 (1987)].
[18]M. E. McIntyre and U.A. Norton, J. Fluid Mech. **212**, 403 (1990).
[19]A. M. Obukhov, Science and Mankind [in Russian], Znanie, M., 1989, p. 96.
[20]A. M. Obukhov, Usp. Matem. Nauk **38**, 101 (1983) [Russ. Math. Surv. **38** (1983)].
[21]V. A. Dovzhenko and F. V. Dolzhanskiĭ, in: Ref. 6, p. 132.
[22]A. M. Obukhov, *Turbulence and the Dynamics of the Atmosphere* [in Russian], Gidrometeoizdat, L., 1988.
[23]J. G. Charney, Geophys. Publ. **17**, 1 (1948).
[24]A. Hasegawa, C. G. McLennan, and Y. Kodama, Phys. Fluids **22**, 2122 (1979).
[25]A. S. Monin and A. M. Obukhov, Izv. Akad. Nauk SSSR, Ser. Geofiz., No. 11, 1360 (1958) [Bull. Acad. Sci. USSR Geophys. Ser. (1958)].
[26]A.S. Monin, Weather Forecasting as a Problem in Physics, MIT Press-,Cambridge, MA, 1972 [Russ. original, Nauka, M., 1965.
[27]A.S. Monin, *Theoretical Principles of Geophysical Hydrodynamics* [in Russian], Gidrometeoizdat, L., 1988.
[28]J. G. Charney, J. Atmos. Sci. **28**, 1087 (1971).
[29]A. P. Mirabel' and A. S. Monin, Izv. Akad. Nauk SSSR Fiz. Atmos. Okeana **16**, 1011 (1980).
[30]A. G. Voronovich and S. A. Rybak, Dokl. Akad. Nauk SSSR **239**, 1457 (1978).
[31]N. N. Romanova, Izv. Akad. Nauk SSSR, Fiz.Atmos. Okeana **23**, 357 (1987).
[32]V. I. Petviashvili, Pis'ma Zh. Eksp. Teor. Fiz. **32**, 632 (1980) [JETP Lett. **32**(11), 619 (1980)].
[33]N. N. Romanova and V. Yu. Tseitlin, Izv. Akad. Nauk SSSR, Fiz. Atmos. Okeana **19**, 796 (1983).
[34]I. Proudman, J. Fluid Mech. **1**, 505 (1956).
[35]K. Stewartson, *ibid.* **3**, 17 (1957).
[36]H. Greenspan, *The Theory of Rotating Fluids*, Cambridge University Press, London, 1969 [Russ. trans., Gidrometeoizdat, Leningrad, 1975].
[37]G. Z. Gershuni, E. M. Zhukhovitskiĭ, and A. A. Nepomnyashchiĭ, *Convective Instability of an Incompressible Liquid* [in Russian], Nauka, M., 1989.
[38]A. M. Obukhov, Dokl. Akad. Nauk SSSR **145**, 1239 (1962) [Sov. Phys. Dokl. 7(8), 682 (1963)].
[39]F. V. Dolzhanskiĭ, Izv. Akad. Nauk SSSR, Fiz. Atmos. Okeana **21**, 383 (1985).
[40]A. T. Zinov'ev and V. N. Shtern, Magn. Gidrodin. (USSR) [Magnetohydrodynamics (USA) **23**, 24 (1987)].
[41]K. A. Sergeev and V. N. Shtern, *ibid.* No. 3, 39 [Magnetohydrodynamics (USA) **23**, 263 (1987)].
[42]L. D. Landau and E. M. Lifshitz, *Electrodynamics of Continuous Media*, Pergamon Press, N. Y., 1960 [Russ. original, Nauka, M., 1957 and *1982*].
[43]E. Lorenz, *Nature and the Theory of the General Circulation of the Atmosphere* (In Russian) Gidrometeoizdat, L., (1970).
[44]E. N. Lorenz, J. Atmos. Sci. **29**, 258 (1972).
[45]F. V. Dolzhanskiĭ, Izv. Akad. Nauk SSSR, Fiz.Atmos. Okeana **23**, 348 (1987).
[46]F. V. Dolzhanskiĭ, *Nonlinear and Turbulent Processes in Physics: Proceedings of the 3rd International Workshop*, April 13–26, Kiev (1987), Vol. 2, p. 25.
[47]F. P. Dolzhanskiĭ, M. V. Kurganskiĭ, and Yu. L. Chernous'ko, Izv. Akad. Nauk SSSR Fiz. Atmos. Okeana **15**, 597 (1979).
[48]Yu. L. Chernous'ko, *ibid.* **16**, 423 (1980) [Izv. Acad. Sci. USSR Atmos. Oceanic Phys. **16**, 285 (1980)].
[49]F. V. Dolzhanskiĭ, *ibid.* **17**, 563 (1981) [Izv. Acad. Sci. USSR Atmos. Oceanic Phys. **17**, 413 (1981)].
[50]C. C. Lin, *Theory of Hydrodynamic Stability*, Cambridge Univ. Press, N. Y., 1955 [Russ. transl., IL, M., 1958].
[51]W. Wasow, Ann. Math. (2) **49**, 852 (1948).
[52]R. Betchov and W. O. Criminale, Stability of Parallel Flows, Academic Press, N. Y., 1967 [Russ. transl., Mir, M., 1971].
[53]L. D. Meshalkin and Ya. G. Sinai, Prikl. Mat. Mekh. **25**, 1140 (1961) [PMM J. Appl. Math. Mech. **25**, 1700 (1961)].
[54]R. Betchov and A. Szewczyk, Phys. Fluids **6**, 1391 (1963).
[55]P. G. Drasin and L. N. Howard, J. Fluid Mech. **14**, 257 (1962).
[56]A. Michalke, *ibid.* **19**, Part 4, 543 (1964).
[57]N. F. Bondarenko, M. Z. Gak, and F. V. Dolzhanskiĭ, Izv. Akad. Nauk SSSR Fiz. Atmos. Okeana **15**, *1017* (*1979*).
[58]V. M. Ponomarev, Izv. Akad. Nauk SSSR, Ser. Mekh. zhidk. gaza, No. 1, 3 (1980) [Fluid Dyn. (USSR) (1980)].
[59]E. B. Gledzer, F. V. Dolzhanskiĭ, and A. M. Obukhov, Systems of the Hydrodynamic Type and Their Applicaitons [in Russian], Nauka, M., 1981.
[60]H. Niino, J. Meteor. Soc. Jpn. **60**, 1001 (1982).
[61]D. Yu. Manin, Izv. Akad. Nauk SSSR Mekh. Zhidk. Gaza, No. 2, 19 (1989) [Fluid Dyn. (USSR) (1989)].
[62]J. W. Miles, J. Fluid Mech. **16**, Part 2, 209 (1963).
[63]L. N. Howard, *ibid.*, Part 3, 333.
[64]F. V. Dolzhanskiĭ, Izv. Akad. Nauk SSSR, Fiz. Atmos Okeana **13**, 201 (1977).
[65]S. M. Vishik and F. V. Dolzhanskiĭ, Dokl. Akad. Nauk SSSR **238**, 1032 (1978).
[66]R. W. Miksad, J. Fluid Mech. **56**, Part 4, 695 ((1972).
[67]A. K. M. F. Hussain, Phys. Fluids **26**, 2816 (1983).
[68]R. Hide and C. W. Titman, J. Fluid Mech. **29**, Part 1, 39 (1967).
[69]H. Niino and N. Misawa, J. Atmos. Sci. **41**, 1992 (1983).
[70]M. Rabaud and Y. Couder, J. Fluid Mech. **136**, 291 (1983).
[71]V. A. Dovzhenko, Yu. V. Novikov, and A. M. Obukhov, Izv. Akad. Nauk SSSR Fiz. Atmos. Okeana **15**, 1199 (1979).
[72]V. A. Dovzhenko, A. M. Obukhov, and V. M. Ponomarev, Izv. Akad. Nauk SSSR, Mekh. Zhidk. Gaza, No. 4, 27 (1981) [Fluid. Dyn. (USSR) (1981)].
[73]V. A. Dovzhenko, V. A. Krymov, and V. M. Ponomarev, Izv. Akad. Nauk SSSR Fiz. Atmos. Okeana **20**, 693 (1984).
[74]V. A. Dovzhenko and V. A. Krymov, *ibid.* **23**, 14 (1987) [Izv. Acad. Sci. USSR Atmos. Oceanic Phys.].
[75]A. M. Batchaev and V. A. Dovzhenko, Dokl. Akad. Nauk SSSR **273**, 582 (1983).
[76]A. M. Batchaev, Izv. Akad. Nauk SSSR, Fiz. Atmos. Okeana **24**, 844 (1988).
[77]V. A. Krymov, Izv. Akad. Nauk SSSR Mekh. Zhidk. Gaza, No. 2, 12 (1989) (Fluid Dyn. (USSR) (1989)].
[78]V. A. Krymov and D. Yu. Manin, Izv. Akad. Nauk SSSR, Fiz. Atmos. Okeana **25**, 234 (1989).
[79]T. Yamagat and R. Kimura, J. Meteor. Soc. Jpn. Ser II **51**, 420 (1973).
[80]D. Yu. Manin and Yu. L. Chernous'ko, Izv. Akad. Nauk SSSR, Fiz. Atmos Okeana **26**, 483 (1990).
[81]J. Sommeria, S. Meyers, and H. Swinney, Nature **331**, 689 (1988).
[82]J. Sommeria, S. Meyers, and H. Swinney, *ibid.*, 689; **337**, 58 (1989).
[83]V. A.Dovzhenko and V. A. Krymov, Izv. Akad. Nauk SSSR, Fiz. Atmos Okeana **19**, 534 (1983).
[84]E. N. Lorenz, J. Atmos. Sci. **20**, 130 (1963).
[85]V. I. Klyatskin, Prikl. Mat. Mekh. **36**, 263 (1972) [J. Appl. Math. Mech. **36** (1972)].
[86]J. S. A. Green, J. Fluid Mech. **62**, Part 2 (1974).
[87]J. T. Stuart, *ibid.* **9**, 353 (1960).
[88]J. Watson, *ibid.*, 371.
[89]S. M. Churilov and I. G. Shikham, *ibid.* **180**, 1 (1987); **194**, 187 (1988).
[90]S. M. Churilov, "Instability of zonal shear flow: soft excitation regime," (In Russian) Preprint No. 1–88, SibIZMIR, Irkutsk (1988).
[91]P. Heurre, J. Mec. T. Appl. (SI), 121 (1983).
[92]I. G. Shikham, J. Fluid Mech. **200**, 425 (1989).
[93]V. I. Yudovich, *Numerical Methods for Solving Problems in Mathematical Physics* [in Russian], Nauka, M., 1966.
[94]V. I. Yudovich, Izv. Akad. Nauk SSSR Mekh. Zhidk. Gaza, 32 (1973) [Fluid Dyn. (USSR) (1973)].

[95]S. O. Belotserkovskiĭ, A. P. Mirabel', and M. A. Chusov, Izv. Akad. Nauk SSSR Fiz. Atmos. Okeana **14**, 11 (1978).
[96]A. A. Nepomnyashchiĭ, Prikl. Mat. Mech. **40**, 886 (1976) [PMM J. Appl. Math. Mech. **40** (1976)].
[97]B. Nikolaenko and Z.-S. She, Topological Fluid Mechanics: Proceedings of IUTAM Symposium, Cambridge, England, August 13–18, 1989 (Eds.) H. K. Moffat and A. Tsinober, 1989, p. 304.
[98]S. Ya. Gertsenshteĭn, Dokl. Akad. Nauk SSSR **231**, 1319 (1976) [Sov. Phys. Dokl. **21**(12), 706 (1976)].
[99]S. Ya. Gertsenshteĭn, E. M. Lezin, and V. Ya. Shkadov in: Abstracts of Reports at the 2nd All-Union Conference on Current Problems in Thermal Convection (In Russian) Perm', 1975, p. 50.
[100]R. E. Esch, J. Fluid. Mech. **3**, Part 3, 289 (1957).
[101]D. Yu. Manin, Izv. Akad. Nauk SSSR Fiz. Atmos. Okeana **25**, 802 (1989).
[102]J. M. Chomaz, M. Rabaud, C. Basdevant, and Y. Couder, J. Fluid Mech. **187**, 115 (1988).
[103]V. A. Krymov, Izv. Akad Nauk SSSR Fiz. Atmos. Okeana **24**, 475 (1988).
[104]H. Niino, J. Meteor. Soc. Japan Ser II **60**, 1024 (1982).
[105]D. Yu. Manin, "The theory of stability of quasi-two-dimensional zonal flows taking into account external friction and rotation," (In Russian) Author's Abstract of Candidate's Dissertation in Physical–Mathematical Sciences, Moscow, 1989.
[106]R. H. Kraichnan, Phys. Fluids 10, No. 7 (1967).
[107]E. J. Hopfinger, J. Mec. Appl. (SI), 21 (1983).
[108]A. S. Monin and A. M. Yaglom, *Statistical Fluid Mechanics*, MIT Press, Cambridge, MA, 1975 [Russ. original, Nauka, M., Part 1, 1965 and Part 2, 1967].
[109]D. Yu. Manin, "On the characteristic size of vortices in developed quasi-two-dimensional flows (In Russian)," Preprint No. 6, Institute of the Physics of the Atmosphere of the Academy of Sciences of the USSR, Moscow (1989).
[110]D. Yu. Manin, Izv. Akad. Nauk SSSR Fiz. Atmos Okeana **26**, No. 6 (1990).
[111]G. S. Golitsyn, *Introduction to theDynamics of Planetary Atmospheres* [in Russian], Gidrometeoizdat, Leningrad, 1973.
[112]H. L. Kuo, J. Meteorol. **6**, 105 (1947).
[113]P. B. Rhines, J. Fluid Mech. **69**, 417 (1975).
[114]V. V. Dolotin and A. M. Fridman, in: *Dynamics of Astrophysical Disks* (Ed.) J. Sellowood, Cambridge University Press, 1989, p. 178.

Translated by M. E. Alferieft